DEVELOPMENT OF A PHYSIOLOGICALLY-BASED PHARMACOKINETIC MODEL OF TRICHLOROETHYLENE AND ITS METABOLITES FOR USE IN RISK ASSESSMENT

Prepared for:

United States Air Force

Prepared by:

USAF-EPA TCE PBPK workgroup

Oct. 14, 2004

USAF-EPA TCE PBPK workgroup members:

Jerry Blancato: U.S. Environmental Protection Agency (EPA)

Weihsueh Chiu**: U.S. Environmental Protection Agency

Harvey J. Clewell*: ENVIRON Health Sciences Institute, Ruston, Louisiana 71270

Tammie R. Covington*: ENVIRON Health Sciences Institute, Ruston, Louisiana 71270

Jeffrey W. Fisher*: University of Georgia, Athens, GA

Eric Hack: Toxicology Excellence for Risk Assessment (*TERA*)

John Lipscomb**: U.S. Environmental Protection Agency

Dave Mattie: Air Force Research Laboratory (AFRL), the Biosciences Protection Division of the Human Effectiveness Directorate (HEPB)

Miles Okino: U.S. Environmental Protection Agency

Fred Power: U.S. Environmental Protection Agency

Qiyu J. Zhao: Toxicology Excellence for Risk Assessment

*: Primary authors
**: Major contributors

PREFACE

The U.S. Air Force (USAF) and the U.S. Environmental Protection Agency (EPA) are jointly sponsoring a scientific workgroup to develop a harmonized PBPK model for TCE and its metabolites based on the full range of available science and data. This workgroup is composed of scientists from the USAF and EPA, with technical expertise from Toxicology Excellence for Risk Assessment (TERA) and other scientists under contract to the USAF. The results of this joint USAF-EPA workgroup will serve as important input to ongoing TCE risk assessment activities, including a planned multi-agency consultation with the National Academy of Sciences on TCE science issues as well as EPA's revised TCE human health risk assessment.

This effort focuses on the scientific data, methods, and uncertainties surrounding the quantitative modeling of absorption, distribution, metabolism, and excretion of TCE and its metabolites through the use of PBPK models. No conclusions as to the human health risks of TCE exposure are being developed as part of this project; and no judgments as to what should or should not be used in risk assessment are being made. While the goal of this project is to develop a harmonized PBPK model based on the best available scientific information, the results of this project may need to be further refined, augmented, and/or modified for use in risk assessment.

DISCLAIMER

This document and the model it describes are drafts for peer consultation purposes only, and have been developed through a U.S. Air Force (USAF) contract to Toxicology Excellence for Risk Assessment (TERA) and subcontracts to ENVIRON and the University of Georgia. USAF and U.S. Environmental Protection Agency (EPA) staff have provided technical input to its development, but it does not necessarily reflect the views or polices of the USAF or the EPA, and no official endorsement should be inferred. Mention of trade names or commercial products does not constitute endorsement or recommendation for use.

ABBREVIATIONS

ACSL	Advanced Continuous Simulation Language
ADH	Alcohol Dehydrogenase
AUC	Area Under the Concentration Curve
BSA	Body Surface Area
CHL	Chloral
CV	Coefficients of Variation
CYP	Cytochrome P450
DCA	Dichloroacetic Acid
DCVC	Dichlorovinylcysteine
GSH	Glutathione
GST	Glutathione Transferase
MCA	Monochloroacetic Acid
MFO	Mixed Function Oxidase (P450)
PBPK	Physiologically Based Pharmacokinetic
TCA	Trichloroacetic Acid
TCE	Trichloroethylene
TCOH	Trichloroethanol
UGT	UDP Glucuronosyl Transferase

ABSTRACT

A physiologically based pharmacokinetic (PBPK) model was developed which provides a comprehensive description of the kinetics of trichloroethylene (TCE) and its metabolites, trichloroethanol (TCOH), and trichloroacetic acid (TCA), in the mouse, rat, and human, for both oral and inhalation exposure. The model includes descriptions of the three principal target tissues for cancer identified in animal bioassays: liver, lung, and kidney. Dose metrics that can be calculated with the model for cancer risk assessment include the area under the concentration curve (AUC) for TCA in the plasma or liver, the peak concentration and AUC for chloral (CHL) in the tracheo-bronchial region of the lung, and the production of a thioacetylating intermediate from dichlorovinylcysteine (DCVC) in the kidney. Additional dose metrics that can be calculated for noncancer risk assessment include the peak concentrations and AUCs for TCE and TCOH in the blood, as well as the total metabolism of TCE divided by the body weight. There is currently no adequate data available with which to confidently parameterize a description for another metabolite of interest, dichloroacetic acid (DCA). Model predictions of TCE, TCA, and TCOH concentrations in rodents and humans are consistent with a variety of experimental data, suggesting that the model should provide a useful basis for evaluating cross-species differences in pharmacokinetics for these chemicals. In the case of the lung and kidney target tissues, however, only limited data are available for establishing cross-species pharmacokinetics. As a result, PBPK model calculations for these dose metrics are highly uncertain.

INTRODUCTION

Physiologically-based pharmacokinetic (PBPK) modeling is widely held to be a useful methodology for improving the accuracy of chemical risk assessment. The goal of PBPK modeling is to simulate the uptake, distribution, metabolism, and elimination of a chemical in an organism, using as realistic a description of the relevant physiology and biochemistry as is necessary and feasible. For its use in risk assessment, PBPK modeling attempts to describe the relationship between external measures of exposure (e.g., amount administered or concentration in air) and internal measures of biologically-effective dose (e.g., amount metabolized or concentration of an active metabolite in the tissue displaying the toxic response) in both the experimental animal and the human.

The most recent EPA cancer risk estimates for trichloroethylene (TCE) were derived in part using PBPK models. In particular, risks of liver cancer based on tumors in mice were estimated using two different PBPK models, [1, 2] as well as with "calibrated" versions of these two models using re-estimated parameters obtained from Markov chain Monte Carlo analysis.[3, 4] The purpose of the study reported here was to develop a single harmonized PBPK model for TCE that included as complete a description as possible of all of the metabolites and target tissues that may be relevant to the toxicity and carcinogenicity of TCE, and to characterize the accuracy and reliability of the resulting model in providing dosimetry estimates in support of a risk assessment for TCE.

Requirements for a PBPK Model to Support TCE Risk Assessments

Recent quantitative cancer risk estimates for TCE have been based on animal bioassays, specifically liver and lung tumors in mice and kidney tumors in rats, as well as

on human epidemiological studies. In the case of the human studies, PBPK modeling can be used to perform route-to-route extrapolation.

For each of the three rodent target tissues, liver, lung, and kidney, there is evidence that the carcinogenicity of TCE may be associated with one or more of its metabolites: trichloroacetic acid (TCA) and dichloroacetic acid (DCA) in the liver, CHL in the lung, and 1,2-DCVC in the kidney. Thus, to be useful in a comprehensive cancer risk assessment for TCE, a PBPK model should include at least three target tissues: liver, lung, and kidney, along with a description of the kinetics of the metabolites that may play a role in the carcinogenic activity.

Several target tissues have also been identified for the noncancer toxicity of TCE, including the liver, kidney, CNS, immune system, and developing fetus. As in the case of the carcinogenicity of TCE, several of these noncancer endpoints appear to be associated with exposure to the metabolites of TCE rather than to the parent chemical itself. For example, trichloroethanol (TCOH), the major metabolite of TCE, has been suggested to be responsible for the observed neurological effects of chloral hydrate.

Previous PBPK Modeling of TCE

A number of PBPK models have been developed for TCE. However, most have only been parent chemical models; that is, they provide a pharmacokinetic description of TCE itself, but do not include an explicit description of the pharmacokinetics of any of the metabolites. Therefore, these parent chemical models cannot be used for predicting tissue exposure to specific metabolites.

Fisher and coworkers developed a PBPK model for TCE and its principal metabolite, TCA, in the rat and mouse.[5] These rodent models, together with a similar model of TCE and TCA in the human,[6] served as the basis for a PBPK-based risk assessment for TCE liver carcinogenicity[7] based on either average daily total metabolism or average daily AUC for TCA. These models provided the first successful cross-species pharmacokinetic description for a metabolite of TCE. Subsequently, Clewell and co-workers built on the work of Fisher and Allen[7] by adding limited descriptions of additional metabolites (TCOH, DCA, CHL, 1,2-DCVC) and target tissues (lung and kidney).[1] Fisher and colleagues also continued to elaborate and refine their PBPK models for TCE, focusing on the metabolites of interest for liver carcinogenicity.[2] Published models include (1) a model of the kinetics of TCE, CHL, TCA, DCA, and TCOH in the B6C3F1 mouse based on data from corn oil gavage exposures,[8] (2) a model of TCE, TCA, and TCOH in the human based on data from controlled human inhalation exposures,[9] (3) a model of TCE, TCA, and TCOH kinetics in the rat that considers enterohepatic recirculation of TCA and TCOH following oral or intravenous exposure to TCE,[10] and (4) a model of inhaled TCE and its oxidative metabolites in the B6C3F1 mouse.[11] A recent study evaluated various elements of the PBPK description in the rat, including diffusion limited uptake in the fat and liver.[12] Together, these models provide a capability for estimating dose metrics in the mouse, rat, and human in support of a risk assessment for TCE liver carcinogenicity. A potential advantage of these more recent mouse PBPK models[8, 11] is that their calibration includes data on TCA concentrations in the liver. However, since there was no human data on liver concentrations, the human

model[9] could not be similarly calibrated. Therefore, the relationship of liver and blood TCA dosimetry must be inferred from data on plasma binding of TCA.[13]

DESCRIPTION OF THE HARMONIZED PBPK MODEL FOR TCE

PBPK Model Structure

The structure of a PBPK model is necessarily a function of several variables: the physicochemical and biochemical properties of the compound, the physiological and functional properties of the biological system, and the experimental scenarios being investigated. In addition, the model must incorporate information on the various metabolites generated from the compound that are of importance for the intended application. The metabolism of TCE is summarized in Figure 1, which is adapted from the review by Lash et al.[14]

A diagram of the PBPK model developed for TCE and its metabolites is shown in Figures 2 and 3.[1] The model was written in acslXtreme (The AEgis Technologies Group, Inc., Austin, Texas), an implementation of the Advanced Continuous Simulation Language (ACSL). The ACSL source code for the model is included in Appendix A. The parent chemical portion of the model (Figure 2a) includes individual tissue compartments for the liver, GI tract tissue, fat, and tracheo-bronchial region of the lungs. All other tissues are lumped into rapidly perfused (kidney, brain, alveolar region of lungs, etc) and slowly perfused (muscle, skin, etc) compartments. The model has the capability to describe the fat compartment as a diffusion-limited tissue (Figure 2b). The model

[1] The diagrams in Figures 2 and 3 are taken directly from the acslXtreme graphic model display. The blocks are color coded. (Red: blood compartment. Dark Blue: venous blood compartment. Yellow: tissue compartment. Brown: metabolism compartment. Light Green: bile compartment. Dark Green: dosing compartment. Purple: excretion compartment. Light blue: submodel. Rose: mass balance compartment.)

includes both inhalation and oral routes of exposure. Oral gavage is modeled using a two-compartment description of the gastrointestinal tract in order to better simulate the timecourse for the uptake of TCE from corn oil gavage. Allometric scaling is used throughout the model (volumes scaled by body weight, flows and metabolic capacities scaled by body weight to the three-quarters power, rate constants scaled by body weight to the negative one-quarter power) to simplify intraspecies and interspecies extrapolation. Parent chemical dose metrics provided in the model include the concentration of TCE in blood and tissues, as well as the AUC for TCE in the blood.

The model includes a number of submodels describing metabolism of TCE as well as downstream metabolism and elimination (Figure 3). These submodels are aimed at providing metabolite dose metrics, including tissue-specific dose metrics for the lung, liver, and kidney target tissues. Except where otherwise noted, Michaelis-Menten kinetics are assumed for all metabolic processes.

Lung Submodel. The tracheo-bronchial region of the lungs, which receives its own arterial blood supply, is described separately to support the modeling of *in situ* metabolism in this region by the Clara cells (Figure 3a). This approach for describing metabolism in the cells lining the airways of the lung was felt to be more biologically accurate than the sequential gas exchange and lung tissue compartments used in the methylene chloride model.[15] However, as long as metabolism in the lung is unimportant for presystemic elimination, as is the case for TCE and methylene chloride, the two descriptions should yield identical results. The dose metrics provided for the lung are the instantaneous concentration and AUC for CHL in the tracheo-bronchial region, which is

assumed to be produced by saturable production and clearance of CHL in Clara cells. No systemic circulation of CHL is considered in the model.

Oxidative Metabolism. Apart from the limited metabolism occurring in the lung, the model assumes that all oxidative metabolism takes place in the liver. The dose metric provided to describe metabolism is the total amount of TCE metabolized divided by the body weight. The model does not actually calculate the formation and metabolism of CHL in the liver, but instead assumes that TCA and TCOH are formed in a fixed yield from the oxidative metabolism of TCE (Figure 3b). In the model, TCOH can subsequently be oxidized to TCA or conjugated with glucuronic acid. Biliary excretion of TCOH glucuronide and enterohepatic recirculation of free TCOH are described, with only the glucuronide being excreted in the urine (Figures 3b-3e). The description of TCA includes compartments for liver, blood, and other tissues, with clearance into the urine from blood (Figure 3f). Binding of TCA in the plasma is modeled using equations derived from experimental data,[13] and only the free TCA is exchanged with the tissues. Tissue distribution is described using measured partitioning of TCA between tissues and blood.[8, 9, 16] Measured partition coefficients for total TCA between tissues and blood were converted to partitions for free TCA between tissues and plasma, assuming that all TCA in the tissue is free and using an estimate of the free fraction in plasma from the in vitro binding studies. An empirical ratio is used to adjust predicted plasma concentrations for comparison with measured blood concentrations. A rudimentary single-compartment description of DCA is included in the model, assuming direct production of DCA from TCE as a constant fraction of the rate of oxidative metabolism (Figure 3g). Dose metrics for use with the liver target tissue include the concentrations

and AUC for TCA in the plasma and liver. The concentration and AUC for TCOH in the blood are also provided as a noncancer dose metric.

Conjugative Metabolism. The model also includes a linear metabolic pathway representing conjugation of TCE by GST (Figure 3b). The model implicitly assumes that all GSH conjugation of TCE in the liver leads eventually to the appearance of DCVC in the kidney. Clearance of DCVC by N-acetyl-transferase into the urine is also modeled (Figure 3h). The dose metric provided in the model for the kidney is the total production of a thioacetylating intermediate from DCVC, divided by the volume of the kidney.

PBPK Model Parameters

The parameters for the model are listed in Table 1 and are discussed in the following section.

Parameters for the Parent Chemical. The physiological parameters, with two exceptions, were based on the recommendations of the ILSI Risk Science Institute Working Group on Physiological Parameters.[17] The exceptions were the cardiac output in the mouse and the alveolar ventilation in the human, which were based on the recommendations of Arms and Travis.[18] In the model, the tissue volumes and blood flows for the gut, liver, and tracheo-bronchial region are subtracted from the values shown for "all rapidly perfused tissues" to obtain the parameters for the rapidly perfused tissue compartment shown in Figure 2, and those for the fat are subtracted from the values shown for "all slowly perfused tissues" to obtain the parameters for the slowly perfused tissue compartment. The kidney volume shown in the table is used only in

calculations for the kidney dose-surrogate; as shown in Figure 2, the kidney is not described separately in the parent chemical model.

The partition coefficients for TCE were obtained from the work of Fisher and Allen;[5-7] the partition coefficients for the gut and tracheo-bronchial tissues were assumed to be the same as those reported for the richly perfused tissues. The oral uptake parameters were estimated from data on the appearance of TCE and its metabolites in the blood following gavage in mice and rats. For some parameters, identified in Table 1, values chosen for calculating risk assessment dose metrics were different from those chosen to reproduce pharmacokinetic data. For example, human dose metrics were calculated using a value for alveolar ventilation of 24, which corresponds to the EPA's standard assumption of a total ventilation rate of 20 m^3/day. Similarly, animals used in pharmacokinetic studies tend to have lower average body weights than animals used in cancer bioassays, so body weights appropriate to each case were used in the model.

Parameters for Oxidative Metabolism. Initial values for the metabolic parameters for TCE were obtained from the work of Fisher and Allen;[5-7] however, the metabolic and clearance parameters for TCA and TCOH were derived primarily on the basis of fitting the pharmacokinetic data depicted in the figures. Since the model contains a large number of metabolic and clearance parameters, many of which are highly correlated, the parameter values estimated by this process (i.e., the kinetic parameters for TCA and TCOH) cannot be considered to be unequivocally identified. However, an additional biological constraint was applied by attempting to ensure that parameters are relatively constant across exposure scenarios within a given species, and (to the extent justified by the experimental data) across species. This constraint greatly reduces the likelihood that

alternative parameterizations could demonstrate equivalent success in reproducing the entire body of data. Another constraint on the parameterization not obvious from the figures is the fact that of the total TCOH extractable from the blood, roughly 80% is present as free TCOH in the human,[19] while roughly 70-85% is present as the glucuronide in the rodent.[20, 21] In the figures in this paper, the model concentrations shown represent either free TCOH or the total of TCOH plus its glucuronide, corresponding to the experimental data provided.

It is informative to note the departures from simple allometric expectations that were required on the basis of the experimental data across species. As with most other xenobiotics, the mouse shows a relatively greater, and more variable, capacity (VMC) for oxidative metabolism of TCE than the rat and human. Moreover, the Km for oxidative metabolism of TCE in the human appears to be roughly an order of magnitude larger than in the rodents. A striking difference between humans and rodents, which was clearly demanded by the experimental data, was that the oxidation of TCOH to TCA appears to be a relatively high affinity, low capacity process in the rodent but low affinity, high capacity in the human. It may be that this disparity reflects the involvement of different enzymes (e.g., MFO in the rodent *vs*. ADH in the human). The result of this species difference is that although the model uses a similar value across species for PO (based on the initial split of TCA and TCOH from CHL), the apparent ratio of TCA to TCOH predicted (and observed) over the entire time-frame of an exposure to TCE is much higher in the human than in the rodent. The apparent capacity for glucuronidation of TCOH in the human, on the other hand, is much lower than in the rodent, as reflected in the greatly different ratios of free TCOH to glucuronide in the blood, mentioned above.

Parameters for Lung Metabolism. The parameters in the PBPK model for predicting the lung dose metric are the capacity and affinity for the production of CHL, and the capacity and affinity for its clearance. In the model, the production of CHL in the tracheobronchial region was assumed to be associated with the P450 activity in that tissue. This is the assumption that was made in the pharmacokinetic risk assessment for methylene chloride.[15] The approach used in that risk assessment was also used to obtain the parameters in this case: the affinity in the lung was assumed to be the same as in the liver for the same species, and the relative capacity of the lung compared to the liver was determined on the basis of P450 activity measured with standard substrates.[15] Based on these data, P450 activity falls off much more rapidly with body weight than would be expected from allometric considerations. No data was available on the clearance of CHL in the lung across species, therefore it was assumed to be a low affinity, high capacity enzyme system such as ADH. The parameters in the PBPK model were chosen such that concentrations of CHL in the lung of the mouse predicted by the model were consistent with those observed in experimental studies.[8] It was further assumed that the clearance of CHL in the lung scales across species according to allometric expectations (i.e., by body weight to the 3/4 power). This assumption leads to much lower CHL concentrations in the lungs of rats and humans compared to mice for the same TCE exposure conditions. An alternative assumption was that the activity of the enzyme responsible for the clearance of CHL scales in the same way as P450; this assumption leads to similar concentrations of CHL in the lungs of mice, rats and humans for the same TCE exposure conditions.

Parameters for Conjugative Metabolism. The parameters in the PBPK model for predicting the kidney dose metric are the production of DCVC by the GST pathway, its activation by beta-lyase, and its clearance by N-acetyl-transferase. First-order rate constants are used because the production of metabolites by the GST pathway is quite low, and saturation of enzyme capacity is unlikely. The capacity and affinity of beta-lyase in the kidney have been measured in both rats and humans.[22] This data was used to estimate the apparent first-order rate constants used in the model. No data was available on the activity of beta-lyase in the mouse, so the relationships between beta-lyase metabolic parameters in mice and rats reported for trichlorovinylcysteine derived from perchloroethyene[23] were assumed to apply for DCVC as well. For N-acetyl-transferase, only specific activity data across species is available.[24] These data were converted to the corresponding rate constants by assuming the affinity of N-acetyl-transferase for DCVC is the same as that measured for beta-lyase in the same species. This assumption is supported by the similarity of the affinities of N-acetyl-transferase and beta-lyase for DCVC in the rat: 3.3 mM and 1.6 mM, respectively.[22, 25]

Finally, measurements of oxidative and conjugative metabolites in the urine following TCE exposure[26] were used to obtain estimates of the GST pathway rate constant. The oxidative pathway was represented by total excretion of TCA plus TCOH, while the conjugative pathway was represented by excretion of 1,2-DCVC. Data from the same study on excretion of 2,2-DCVC was not used. Unlike 1,2-DCVC, there was no evidence of a dose-response for 2,2-DCVC as a function of TCE exposure in humans or rodents; similar amounts of 2,2-DCVC were excreted for TCE exposures ranging from 40 to 160 ppm. The results of this analysis[1] indicated that the model could be made to agree

quite well with the urinary data when allometric scaling was assumed for conjugative metabolism.

RESULTS

The predictions of the PBPK model for the experimental data sets used in its development are shown in Figures 4-17. The order of the figures follows the order of use of the data in model development. Mouse data sets are shown first, followed by rat and human.

Figure 4 shows the ability of the model to simulate the chamber concentration time-course in gas-uptake studies conducted with male (a) and female (b) B6C3F1 mice. These data were used to obtain initial estimates of the kinetic parameters for TCE.[5] The resulting estimates of VmaxC were 32.7mg/hr/kg$^{3/4}$ for the male and 23.2 mg/hr/kg$^{3/4}$ for the female. Fractional fat volumes of 0.05 and 0.1 were also estimated for males and females, respectively, based on the early uptake in these studies. It was only possible to determine that Km was probably less than 1ug/L. Estimates of the other kinetic parameters were obtained using data on concentrations of TCE and its metabolites in male mice following oral gavage in corn oil[27] and water[20] vehicles. The resulting fits of the model to the data are shown in Figures 5 and 6. In fitting these two data sets, it was only necessary to use different values for three of the model kinetic parameters. The simulation of the corn oil gavage data was obtained with kAD=0.3, VmaxC=50, and VmaxTCOHC=2, while the aqueous vehicle data was best simulated with kAD=1.0, VmaxC=60, and VmaxTCOHC=0.5. For both data sets, it was also necessary to reduce QPC to 18 L/hr/kg$^{3/4}$, rather than the value of 30 L/hr/kg$^{3/4}$ used in the closed chamber

studies. The rest of the model parameters were as shown in Table 1. Figure 7 shows the predictions of the model for inhalation exposures to TCE in male and female mice.[5] All of the model parameters in this case were those shown in Table 1, except that for the females the value of VmaxC was reduced to 23.2 mg/hr/kg$^{3/4}$ and the urinary excretion rate constant for TCA, kUrnTCAC, was doubled to 0.6 kg$^{1/4}$/hr. The lower value of QPC mentioned above was also used. Validation of these mouse parameter values, shown in Figure 8 was performed using the more recent inhalation data of Greenberg et al.[11]. Finally, the model parameters in Table 1 were tested by using them in the model to predict the time-course for TCE and TCA in a number of tissues for comparison with the corn oil gavage data collected by Abbas et al.[8]; the results of the prediction are displayed in Figure 9. The blind predictions of the model are generally within a factor of two of the data, although the model tends to underestimate TCE concentrations at early times. The model also overestimates liver concentrations of TCA to a much greater extent than blood concentrations, suggesting that the *in vitro* partitioning of TCA may not accurately predict its distribution *in vivo*.

The parameterization of the model in the rat followed a similar approach to that just presented for the mouse. Figure 10 shows the simulation of the gas uptake data for male rats;[28] the resulting estimate of VmaxC was 11.2 mg/hr/kg$^{3/4}$. Estimates of the other kinetic parameters were obtained using data on concentrations of TCE and its metabolites in male rats following oral gavage in corn oil[27] and water[29] vehicles. The resulting fits of the model to these data sets are shown in Figures 11 and 12. In fitting these two data sets, it was only necessary to use different values for two of the model kinetic parameters. The simulation of the corn oil gavage data was obtained with

FracTCE=0.04 and VMaxGlucC=100, while the aqueous vehicle data was best simulated with FracTCE=0.02 and VmaxGlucC=20. The rest of the model parameters were as shown in Table 1 for both simulations. Figure 13 shows the predictions of the model for inhalation exposures to TCE in male and female rats.[5] All of the model parameters in this case were those shown in Table 1 except that for the females the value of VmaxC was increased to 20 mg/hr/kg$^{3/4}$ and the alveolar ventilation rate was decreased to 15 L/hr/kg$^{3/4}$.

Parameterizing the human model is complicated by the fact that inter-individual variation tends to be greater in humans than in in-bred experimental animals. In particular, three of the parameters in the model were found to vary significantly across studies: VmaxC, the capacity of the oxidative metabolism of TCE, VmaxTCOHC, the capacity of the oxidative metabolism of TCOH, and kUrnTCAC, the rate constant for excretion of TCA. The greatest variation was found for VmaxC; values needed to simulate different experimental subjects ranged from 1.5 to 18 mg/hr/kg$^{3/4}$. This 10-fold variation is consistent with other observations of the variability in CYP2E1 metabolism in humans. The variation in the value of kUrnTCAC was similar, ranging from 0.05 to 0.6 kg$^{1/4}$/hr, while that for VmaxTCOHC was not as great, with values ranging from 12 to 40 mg/hr/kg$^{3/4}$. The results of fitting several published human studies[9, 19, 30-32] are shown in Figures 14 – 19. The caption to each figure shows the values of the three parameters discussed above that were used to obtain the simulation displayed.

PBPK Model Validation

The validity of the model for its intended purpose must be evaluated on the basis of the comprehensiveness of its predictive power and the reasonableness of the parameters used to fit the various data sets. The approach for obtaining an initial parameterization of the PBPK model for TCE has already been discussed. This preliminary version of the model is able to reproduce data on TCE and TCA kinetics in the mouse, rat, and human, for both inhalation exposure and oral gavage. In addition, the model is able to describe TCOH kinetics in mice, rats, and humans. No suitable data were available for validation of the model predictions for CHL in the lung, DCVC in the kidney, or DCA in the liver.

It was not possible to obtain complete agreement between the model and each of the studies investigated using a single set of parameters in each species. This failure undoubtedly results from a combination of variation across individuals and animal strains, experimental error, and model error. Nevertheless, given the general agreement of the model with a variety of data on TCE, TCA, and TCOH concentration time-courses in both rodents and humans, there can be relatively high confidence in dose metrics based on the predictions of the PBPK model for these chemicals. Unfortunately, as mentioned earlier, there is a lack of similar data to provide confidence in the model predictions for DCVC in the kidney, CHL in the lung, and DCA in the liver.

DISCUSSION

The harmonized model works reasonably well, considering the variety of data sets it is required to simulate, but it's still in a preliminary state. Final estimates of parameters

should be obtained using Markov chain Monte Carlo analysis, similar to previous studies.[3, 4] There are a number of issues associated with the development of a comprehensive PBPK model for TCE. Several issues that are particularly relevant to the application of a PBPK model in a risk assessment for TCE are discussed below.

It no longer appears feasible to model the kidney pathway. Recent data (Larry Lash, personal communication) suggest that direct excretion of DCVC into the urine and metabolism of DCVC in the kidney by flavin mono-oxygenases (FMO) are significant factors in the human. Moreover, metabolism by FMO produces a reactive metabolite different from the thioketene produced by beta-lyase, so it is not possible to assume that the simple description in the current model would be conservative (protective of human health).

Experimental data on CHL in the mouse[8] indicate that local generation of CHL is the dominant source of the lung concentrations of CHL observed in those studies. In fact, the concentrations of chloral in the lung following oral dosing with TCE were much greater than the concentrations in the blood. Moreover, there is no data with which to parameterize a description of CHL production in the human liver, although local metabolism would be expected to dominate at low environmental exposures. For these reasons, the model does not include CHL in the description of the liver compartment in any species. Nevertheless, the use of the local-metabolism based lung CHL description may still be questionable unless it is possible to resolve uncertainties as to the cross-species scaling of production (i.e., assumptions regarding the relationship between in vitro P450 activity and regional lung metabolic capacity and the relative affinity between

the liver and the lung) and clearance (i.e., the question of ADH or related activities in the lung across species).[1]

Given the problems with the currently available data,[33-35] it is not possible to model the production of DCA from TCE with any confidence. As shown in figures 6, 18, amd 19, an attempt was made to model DCA with a simple one-compartment model, using the empirical volumes of distribution and half lives.[36-41] The production of DCA, which was assumed to represent a constant fraction of the rate of oxidative metabolism, was then estimated from fitting of the limited data in mice and humans on DCA concentrations following exposure to TCE.[9, 20] However, the resulting predicted time-course for DCA after TCE dosing in the mouse was not consistent with the available data.[8, 20] Using the DCA half-life measured in naïve animals (0.05 hours),[41] the model predicted that DCA would be cleared much more rapidly than observed in the studies. Better results were obtained when a half-life of 0.3 hours, representative of an animal in which DCA metabolism had been inhibited,[41] was used (Figure 6). However, for the more recent data,[8] which was collected in such a way as to minimize *ex vivo* conversion of TCA to DCA, the predictions of the model still greatly over-estimated the clearance of DCA as compared to the observed behavior. In fact, the concentrations of DCA measured in this study paralleled those of TCA, suggesting that DCA was being generated from TCA *ex vivo* (rather than from TCE *in vivo*) at a level of about 2%.

Conclusions

The PBPK model described in this paper provides reasonably accurate estimates of dose metrics based on TCE and its major metabolites, TCA and TCOH, in both

experimental animals and humans. Tissue dose metrics calculated with the model should therefore be useful in risk assessments for endpoints where the mode of action involves tissue exposure to these chemicals. Other target tissue dose metrics which can be calculated with the model, including CHL in the lung and DCVC in the kidney, are highly uncertain due to a lack of adequate pharmacokinetic data across species. There is currently no adequate data available with which to confidently parameterize a description of DCA. Additional studies could greatly reduce the uncertainty associated with these dose metrics and make their use in risk assessments more viable.

REFERENCES

1. **Clewell, H.J., Gentry, P.R., Allen, B.C., Covington, T.R., and Gearhart, J.M.,** Development of a physiologically based pharmacokinetic model of trichloroethylene and its metabolites for use in risk assessment. *Environ. Health Perspect.,* 108((suppl 2)), 283-305, 2000.

2. **Fisher, J.W.,** Physiologically based pharmacokinetic models for trichloroethylene and its oxidative metabolites. *Environ. Health Perspect.,* 108 (suppl 2), 265-273, 2000.

3. **Bois, F.Y.,** Statistical analysis of Clewell et al. PBPK model of trichloroethylene kinetics. *Environ. Health Perspect.,* 108(Suppl 2), 307-316, 2000.

4. **Bois, F.Y.,** Statistical analysis of Fisher et al. PBPK model of trichloroethylene kinetics. *Environmental Health Perspectives*, 108, 275-282, 2000.

5. **Fisher, J.W., Gargas, M.L., Allen, B.C., and Andersen, M.E.,** Physiologically based pharmacokinetic modeling with trichloroethylene and its metabolite, trichloroacetic acid, in the rat and mouse. *Toxicol. Appl. Pharmacol.,* 109, 183-195, 1991.

6. **Allen, B.D. and Fisher, J.W.,** Pharmacokinetic modeling of trichloroethylene and trichloroacetic acid in humans. *Risk Anal.,* 13, 71-86, 1993.

7. **Fisher, J.W. and Allen, B.C.,** Evaluating the risk of liver cancer in humans exposed to trichloroethylene using physiological models. *Risk Anal.,* 13, 87-95, 1993.

8. **Abbas, R. and Fisher, J.W.,** A physiologically based pharmacokinetic model for trichloroethylene and its metabolites, chloral hydrate, trichloroacetate, dichloroacetate, trichloroethanol, and trichloroethanol glucuronide in B6C3F1 mice. *Toxicol. Appl. Pharmacol.,* 147, 15-30, 1997.

9. **Fisher, J.W., Mahle, D.A., and Abbas, R.,** A human physiologically based pharmacokinetic model for trichloroethylene and its metabolites, trichloroacetic acid and free trichloroethanol. *Toxicol. Appl. Pharmacol.,* 152, 339-359, 1998.

10. **Stenner, R.D., Merdink, J.L., Fisher, J.W., and Bull, R.,** Physiologically-based pharmacokinetic model for trichloroethylene considering enterohepatic recirculation of major metabolites. *Risk Anal.,* 18(3), 261-269, 1998.

11. **Greenberg, M.S., Burton, G.A., and Fisher, J.W.,** Physiologically based pharmacokinetic modeling of inhaled trichloroethylene and its oxidative metabolites in B6C3F1 mice. *Toxicol. Appl. Pharmacol.,* 154, 264-278, 1999.

12. **Keys, D.A., Bruckner, J.V., Muralidhara, S., and Fisher, J.W.,** Tissue dosimetry expansion and cross-validation of rat and mouse physiologically based pharmacokinetic models for trichloroethylene. *Toxicol Sci*, 76(1), 35-50, 2003.

13. **Lumpkin, M.H., Dallas, C.E., Bruckner, J.V., and Fisher, J.W.,** Physiologically based pharmacokinetic modeling of species-specific effects of plasma binding of trichloroacetic acid from trichloroethylene in mice, rats, and humans. *Toxicologist*, 72(S-1), 867, 2003.

14. **Lash, L.H., Fisher, J.W., Lipscomb, J.C., and Parker, J.C.,** Metabolism of trichloroethylene. *Environ. Health Perspect.*, 108(Suppl 2), 177-200, 2000.

15. **Andersen, M.E., Clewell, H.J., Gargas, M.L., Smith, F.A., and Reitz, R.H.,** Physiologically based pharmacokinetics and the risk assessment process for methylene chloride. *Toxicol. Appl. Pharmacol.*, 87, 185-205, 1987.

16. **Jepson, G.W., Hoover, D.K., Black, R.K., McCafferty, J.D., Mayhle, D.A., and Gearhart, J.M.,** A partition coefficient determination method for nonvolatile chemicals in biological tissues. *Fundamental and Applied Toxicology*, 22, 519-524, 1994.

17. **Brown, R.P., Delp, M.D., Lindstedt, S.L., Rhomberg, L.R., and Beliles, R.P.,** Physiological parameter values for physiologically based pharmacokinetic models. *Toxicol Ind Health*, 13, 407-484, 1997.

18. **U.S. Environmental Protection Agency (USEPA),** *Reference physiological parameters in pharmacokinetic modeling*, EPA/600/6-88/004, Office of Research and Development, Washington, DC, 1988.

19. **Muller, G., Spassovski, M., and Henschler, D.,** Metabolism of trichloroethylene in man. II. Pharmacokinetics of metabolites. *Arch. Toxikol.*, 32, 283-295, 1974.

20. **Templin, M.V., Parker, J.C., and Bull, R.J.,** Relative formation of dichloroacetate and trichloroacetate from trichloroethylene in male B6C3F1 mice. *Toxicol. Appl. Pharmacol.*, 123, 1-8, 1993.

21. **Templin, M.V., Stevens, D.K., Stenner, R.D., Bonate, P.L., Tuman, D., and Bull, R.J.,** Factors affecting species differences in the kinetics of metabolites of trichloroethylene. *J. Toxicol. Environ. Health*, 44, 435-447, 1995.

22. **Lash, L.H., Nelson, R.M., Van Dyke, R.A., and Anders, M.W.,** Purification and characterization of human kidney cytosolic cysteine conjugate beta-lyase activity. *Drug Metab. Dispos.*, 18, 50-54, 1990.

23. **Green, T., Odum, J., Nash, J.A., and Foster, J.R.,** Perchloroethylene-induced rat kidney tumors: an investigation of the mechanisms involved and their relevance to humans. *Toxicol. Appl. Pharmacol.*, 103, 77-89, 1990.

24. **Birner, G., Vamvakas, S., Dekant, W., and Henschler, D.,** Nephrotoxic and genotoxic N-acetyl-S-dichlorovinyl-L-cysteine is a urinary metabolite after occupational 1,1,2-trichloroethylene exposure in humans: implications for the risk of trichloroethylene exposure. *Environ. Health Perspect.*, 99, 281-284, 1993.

25. **Elfarra, A.A., Lash, L.H., and Anders, M.W.,** Metabolic activation and detoxication of nephrotoxic cysteine and homocysteine S-conjugates. *Proc. Nat. Acad. Sci.*, 83, 2667-2671, 1986.

26. **Bernauer, U., Birner, G., Dekant, W., and Henschler, D.,** Biotransformation of trichloroethylene: Dose-dependent excretion of 2,2,2-trichlor-metabolites and mercapturic acids in rats and humans after inhalation. *Arch. Toxicol.*, 70(6), 338-346, 1996.

27. **Prout, M.S., Provan, W.M., and Green, T.,** Species differences in response to trichloroethylene. *Toxicol. Appl. Pharmacol.*, 79, 389-400, 1985.

28. **Andersen, M., Gargas, M., Clewell, H., III, and Severyn, K.,** Quantitative evaluation of the metabolic interactions between trichloroethylene and 1,1-dichloroethylene in vivo using gas uptake methods. *Toxicology and Applied Pharmacology*, 89(2), 149-57, 1987.

29. **Larson, J.L. and Bull, R.J.,** Species differences in the metabolism of trichloroethylene to the carcinogenic metabolites trichloroacetate and dichloroacetate. *Toxicol. Appl. Pharmacol.*, 115, 278-285, 1992.

30. **Muller, G., Spassovski, M., and Henschler, D.,** Metabolism of trichloroethylene in man. III. Interaction of trichloroethylene and ethanol. *Arch. Toxikol.*, 33, 173-189, 1975.

31. **Monster, A., Boersma, G., and Duba, W.,** Kinetics of trichloroethylene in repeated exposure of volunteers. *Int Arch Occup Environ Health*, 42, 283-292, 1979.

32. **Stewart, R., Dodd, H., Gay, H., and Erley, D.,** Experimental human exposure to trichloroethylene. *Arch Environ Health*, 20, 64-71, 1970.

33. **Barton, H., Bull, R., Schultz, I., and Andersen, M.,** Dichloroacetate (DCA) dosimetry: interpreting DCA-induced liver cancer dose response and the potential for DCA to contribute to trichloroethylene-induced liver cancer. *Toxicology Letters*, 106(1), 9-21, 1999.

34. **Ketcha, M.M., Stevens, D.K., Warren, D.A., Bishop, C.T., and Brashear, W.T.,** Conversion of trichloroacetic acid to dichloroacetic acid in biological samples. *J. Anal. Toxicol.*, 20, 236-241, 1996.

35. **Merdink, J.L., Gonzalez-Leon, A., Bull, R.J., and Schultz, I.R.,** The extent of dichloroacetate formation from trichloroethylene, chloral hydrate, trichloroacetate, and trichloroethanol in B6C3F1 mice. *Toxicol. Sci.*, 45, 33-41, 1998.

36. **Curry, S.H., Chu, P.-I., Baumgartner, T.G., and Stacpoole, P.W.,** Plasma concentrations and metabolic effects of intravenous sodium dichloroacetate. *Clin. Pharmacol. Ther.*, 37, 89-93, 1985.

37. **Curry, S.H., Lorenz, A., Chu, P.-I., Limacher, M., and Stacpoole, P.W.,** Disposition and pharmacodynamics of dichloroacetate (DCA) and oxalate following oral DCA doses. *Biopharm. Drug Dispos.*, 12, 375-390, 1991.

38. **Lukas, G., Vyas, K.H., Brindle, S.D., LeSher, A.R., and Wagner, W.E.,** Biological disposition of sodium dichloroacetate in animals and humans after intravenous administration. *J. Pharmaceu. Sci.*, 69, 419-421, 1980.

39. **Lin, E., Mattox, J., and Daniel, F.,** Tissue distribution, excretion, and urinary metabolites of dichloroacetic acid in the male Fischer 344 rat. *J Toxicol Environ Health*, 38, 19-32, 1993.

40. **Saghir, S.A. and Schultz, I.R.,** Low-dose pharmacokinetics and oral bioavailability of dichloroacetate in naive and GST-zeta-depleted rats. *Environ Health Perspect*, 110(8), 757-63, 2003.

41. **Schultz, I.R., Merdink, J.L., Gonzalez-Leon, A., and Bull, R.J.,** Dichloroacetate toxicokinetics and disruption of tyrosine catabolism in B6C3F1 mice: dose-response relationships and age as a modifying factor. *Toxicology*, 173(3), 229-47, 2002.

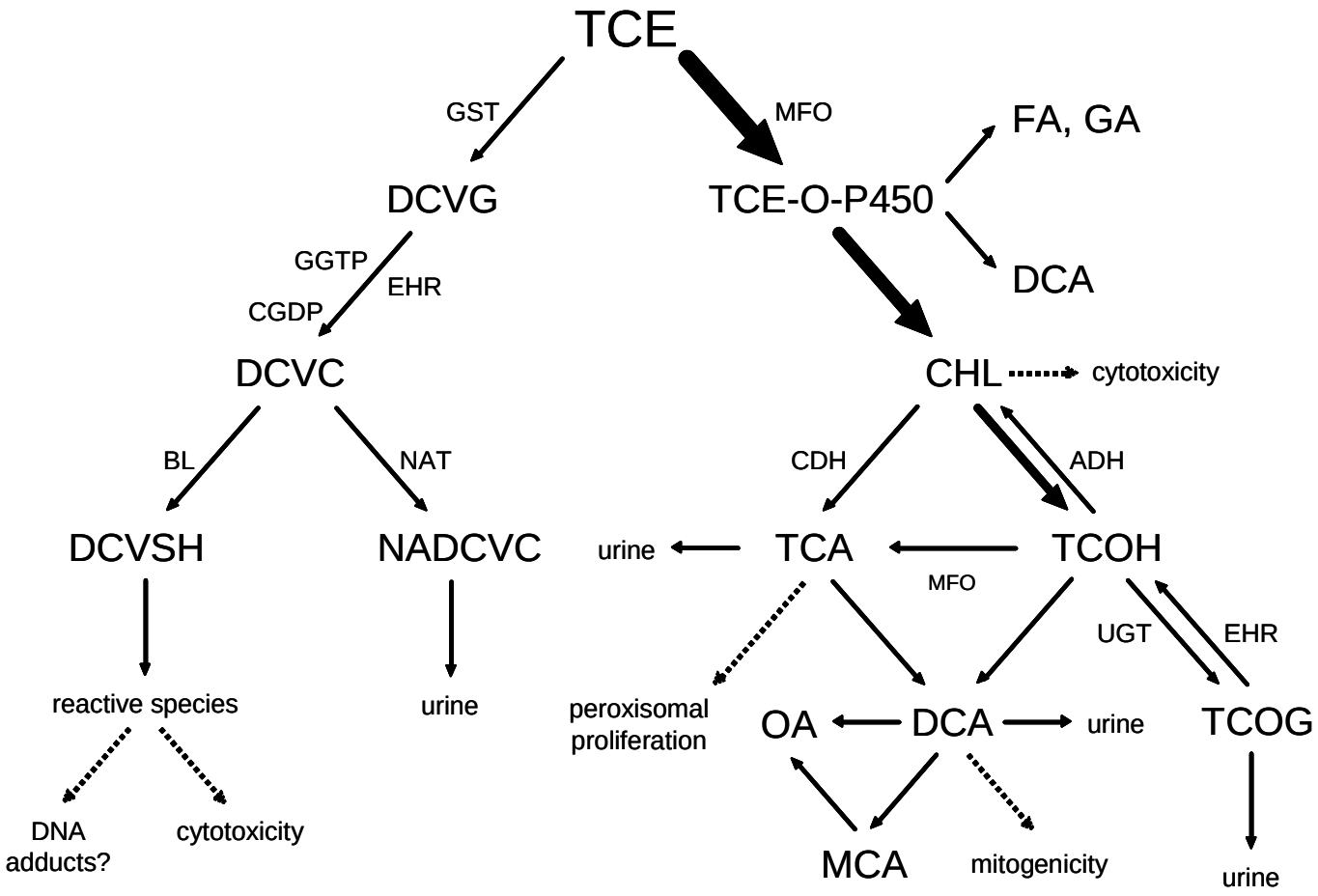

Figure 1: Metabolism of TCE. Abbreviations not given in text: (right pathway) CDH: chloral dehydrogenase (aldehyde oxidase); EHR: enterohepatic recirculation; FA: formic acid; GA: glyoxylic acid; OA: oxalic acid; TCE-O-P450: oxygenated TCE-Cytochrome P450 transition state complex; TCOG: TCOH glucuronide; UGT: UDP glucuronosyl transferase; (left pathway) BL: cysteine conjugate -lyase; CGDP: cysteinyl-glycine dipeptidase; DCVG: dichlorovinyl glutathione; DCVSH: dichlorovinyl mercaptan; GGTP: -glutamyl transpeptidase; NADCVC: N-acetyl dichlorovinylcysteine; NAT: N-acetyl transferase.

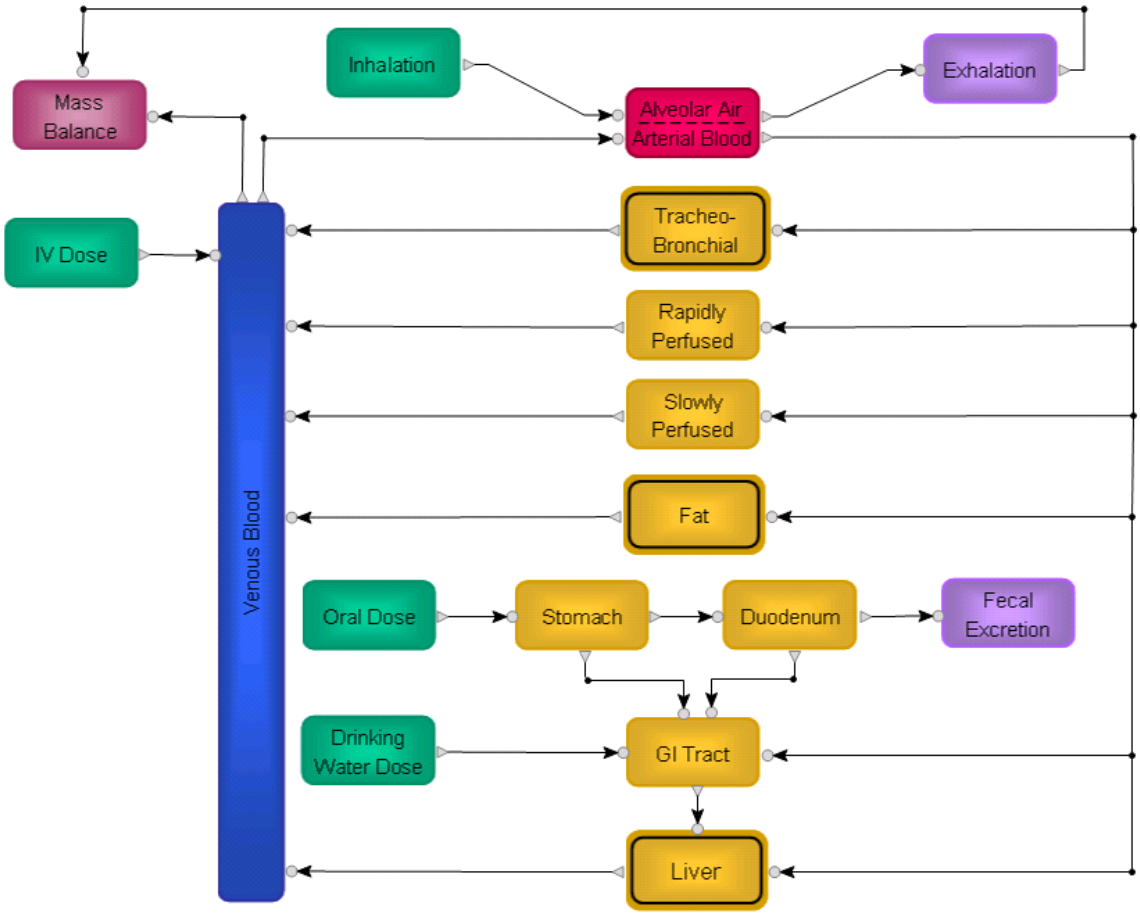

Figure 2a: Model Schematic for Parent Chemical.

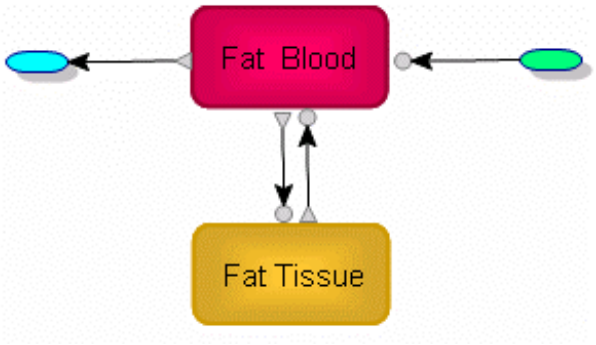

Figure 2b: Sub-Model for Fat Compartment

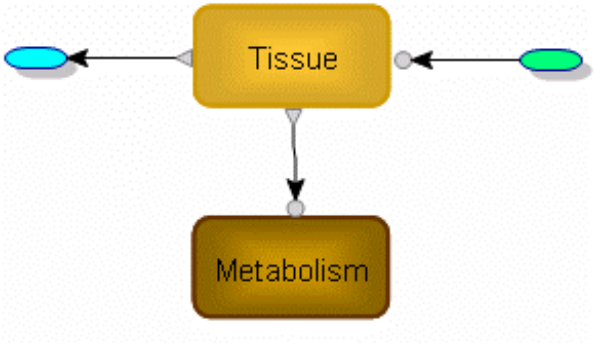

Figure 3a: Sub-Model for Tracheo-Bronchial Compartment

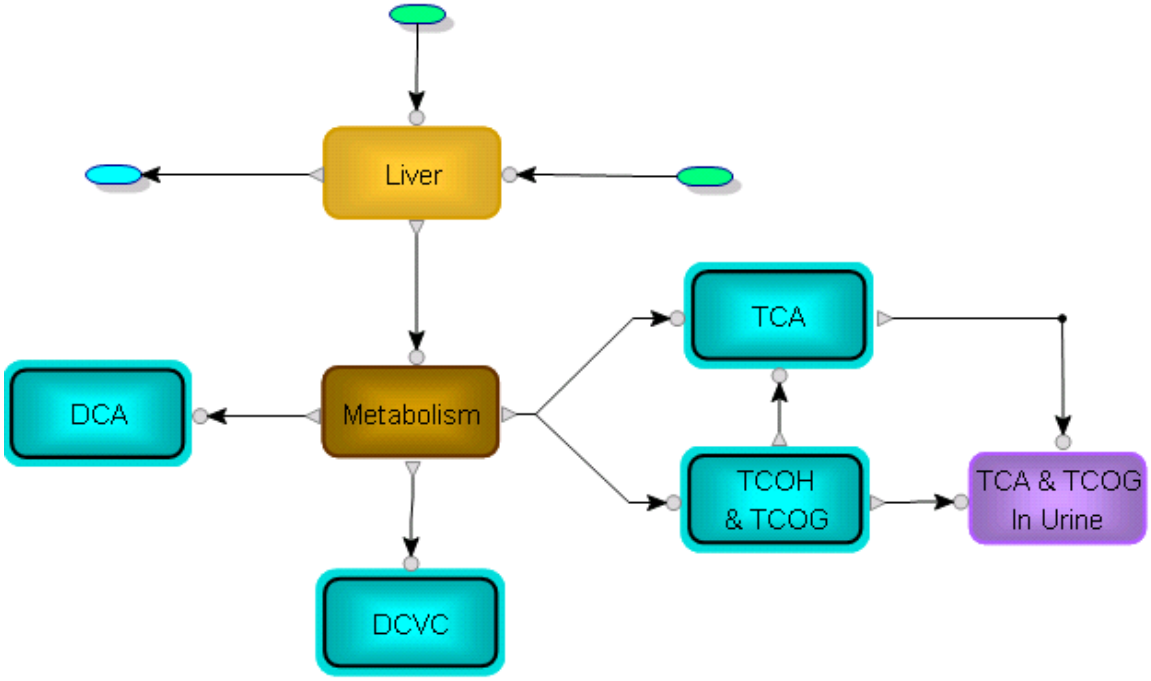

Figure 3b: Sub-Model for Liver

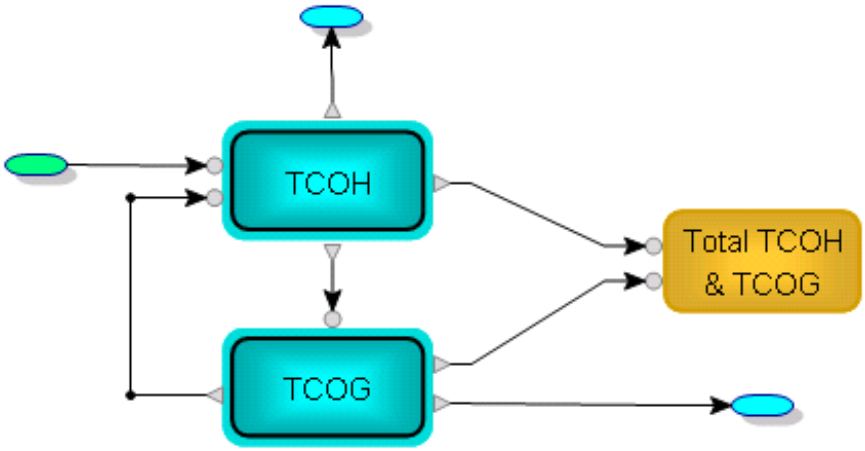

Figure 3c: Sub-Model for TCOH and TCOG

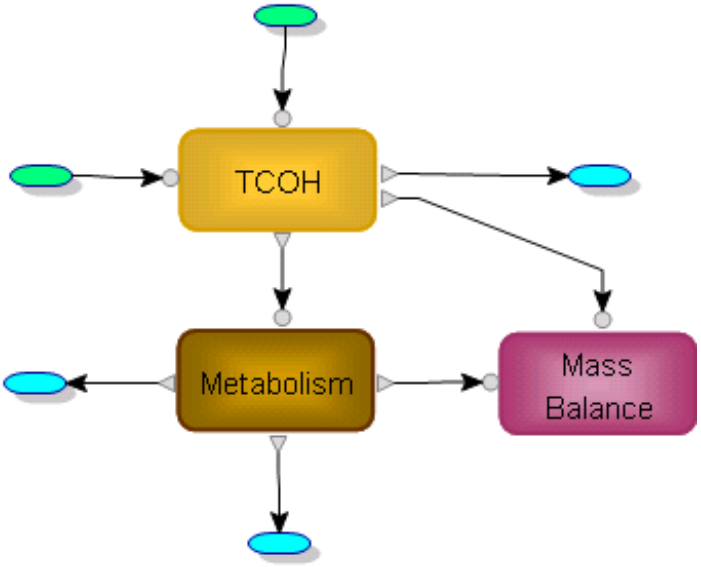

Figure 3d: Sub-Model for TCOH

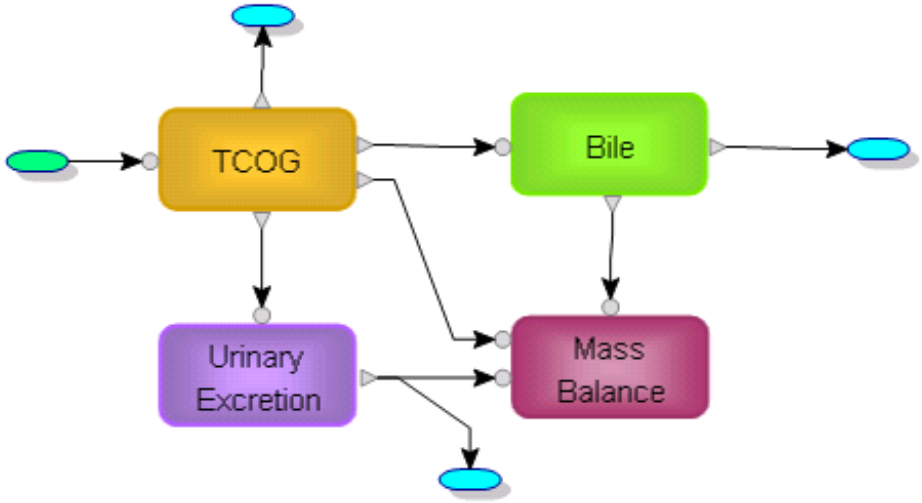

Figure 3e: Sub-Model for TCOG

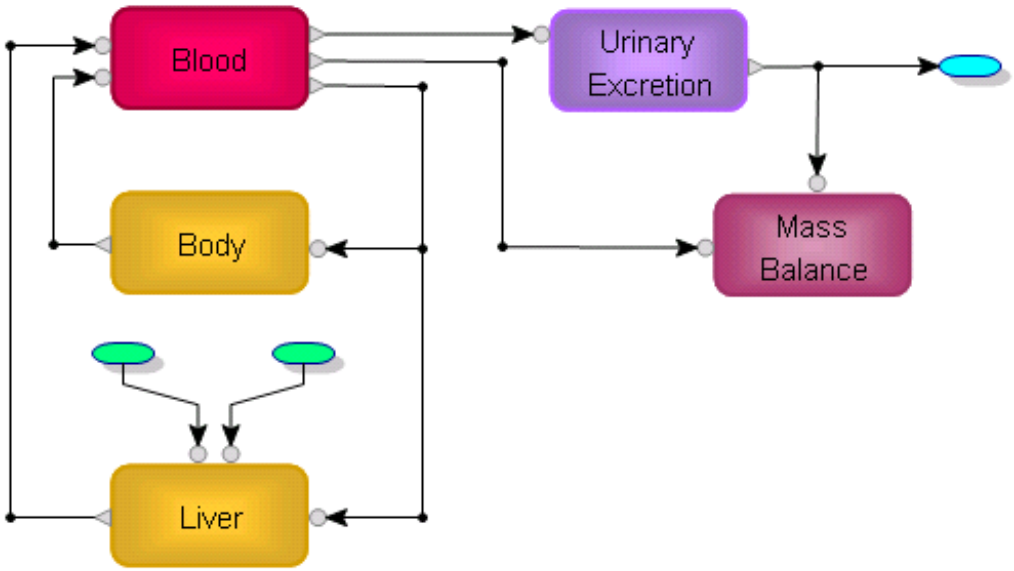

Figure 3f: Sub-Model for TCA

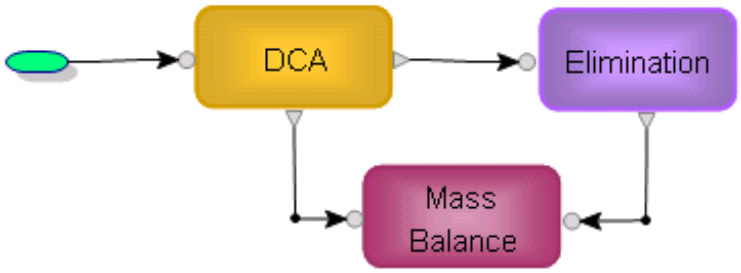

Figure 3g: Sub-Model for DCA

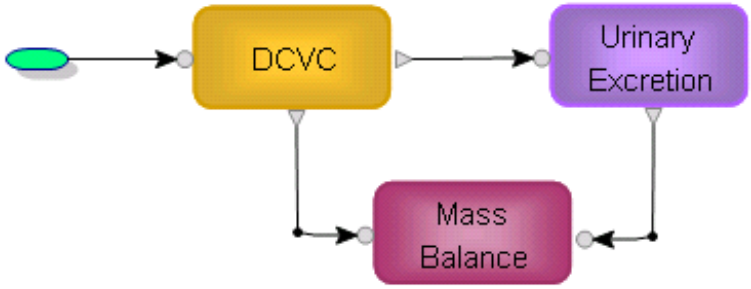

Figure 3h: Sub-Model for DCVC

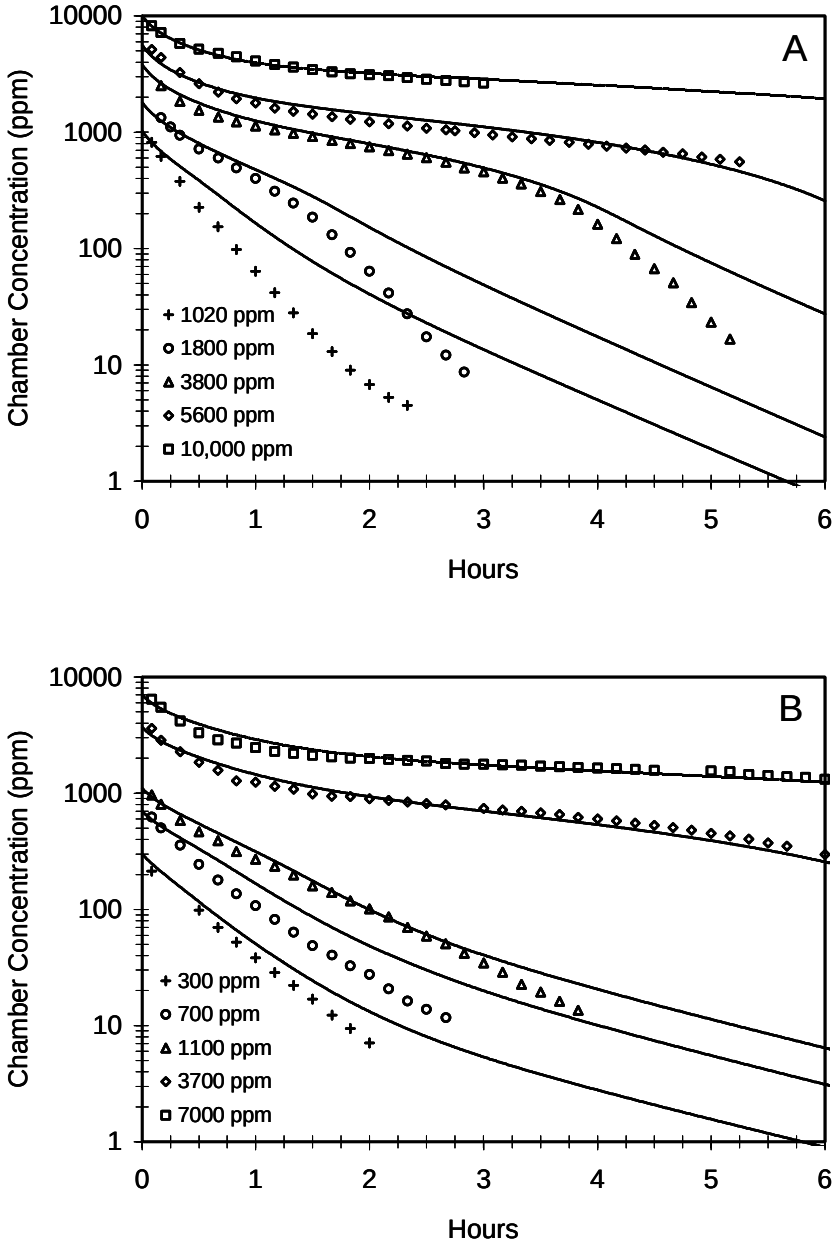

Figure 4. Comparison of predicted and experimental chamber concentrations of TCE in male (A) and female (B) B6C3F1 mice exposed to TCE in a closed, recirculating chamber. Kinetic data are taken from Fisher et al.[5]

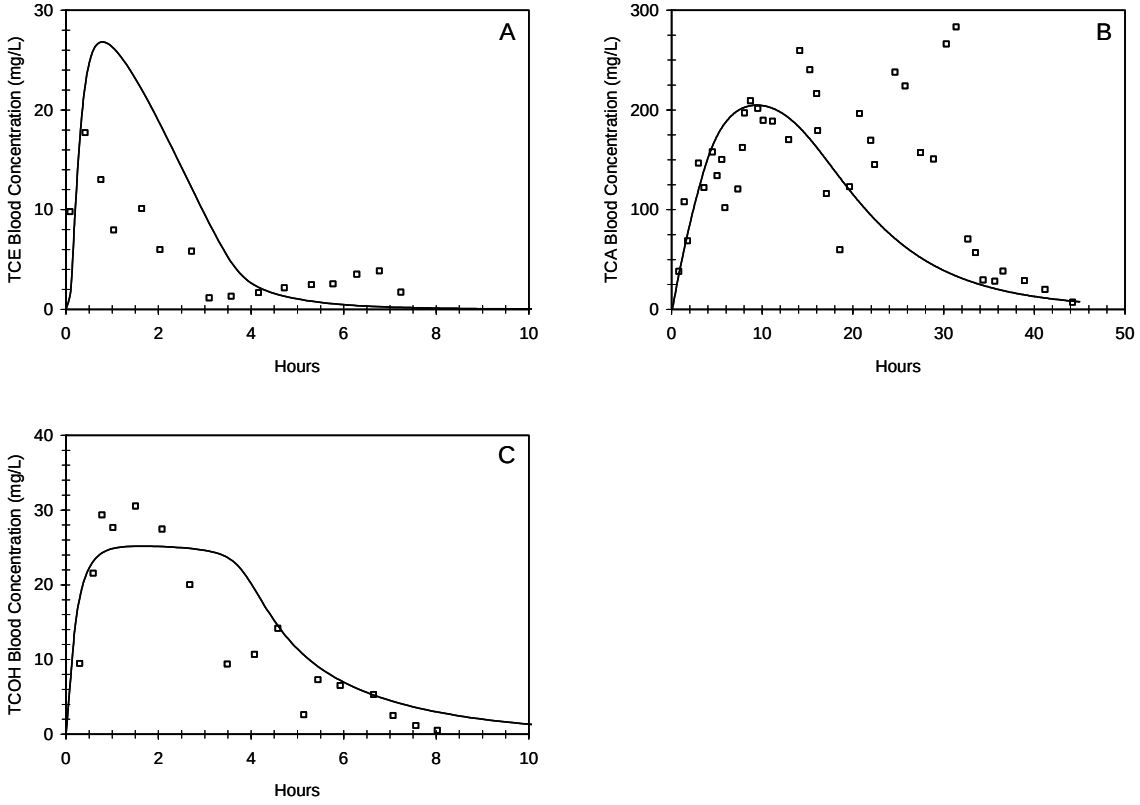

Figure 5. Mean observed and predicted blood concentrations of TCE (A), TCA (B), and free TCOH (C) following corn oil gavage with 1000 mg/kg TCE in mice. Kinetic data are taken from Prout et al.[27]

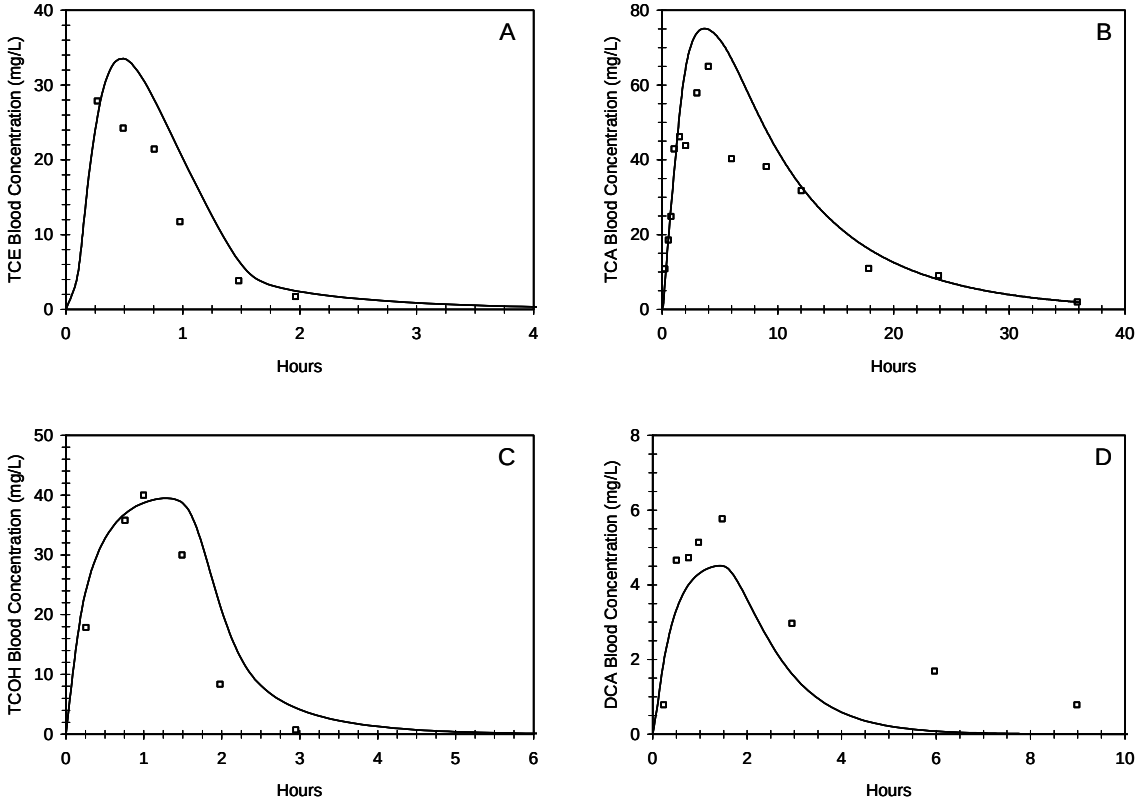

Figure 6. Mean observed and predicted blood concentrations of TCE (A) and metabolites TCA (B), and TCOH (C), and DCA (D) following an oral dose of 499 mg/kg TCE in B6C3F1 mice. Kinetic data are taken from Templin *et al.*[20]

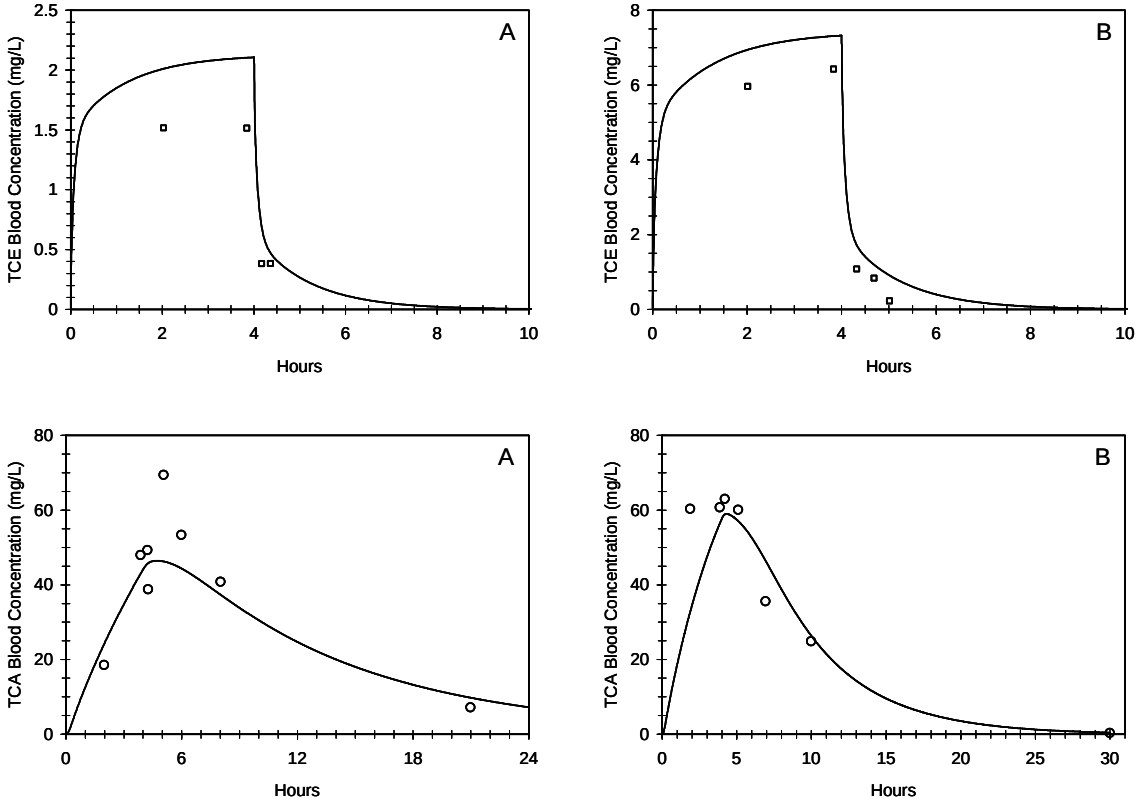

Figure 7. Comparison of predicted and experimental concentrations of TCE in blood and TCA in plasma in B6C3F1 mice exposed to TCE by inhalation. The figures show TCE-blood and TCA-plasma concentrations in (A) male mice exposed for 4 hr to 110 ppm TCE vapors and (B) female mice exposed for 4 hr to 368 ppm TCE vapors. Kinetic data are taken from Fisher et al.[5]

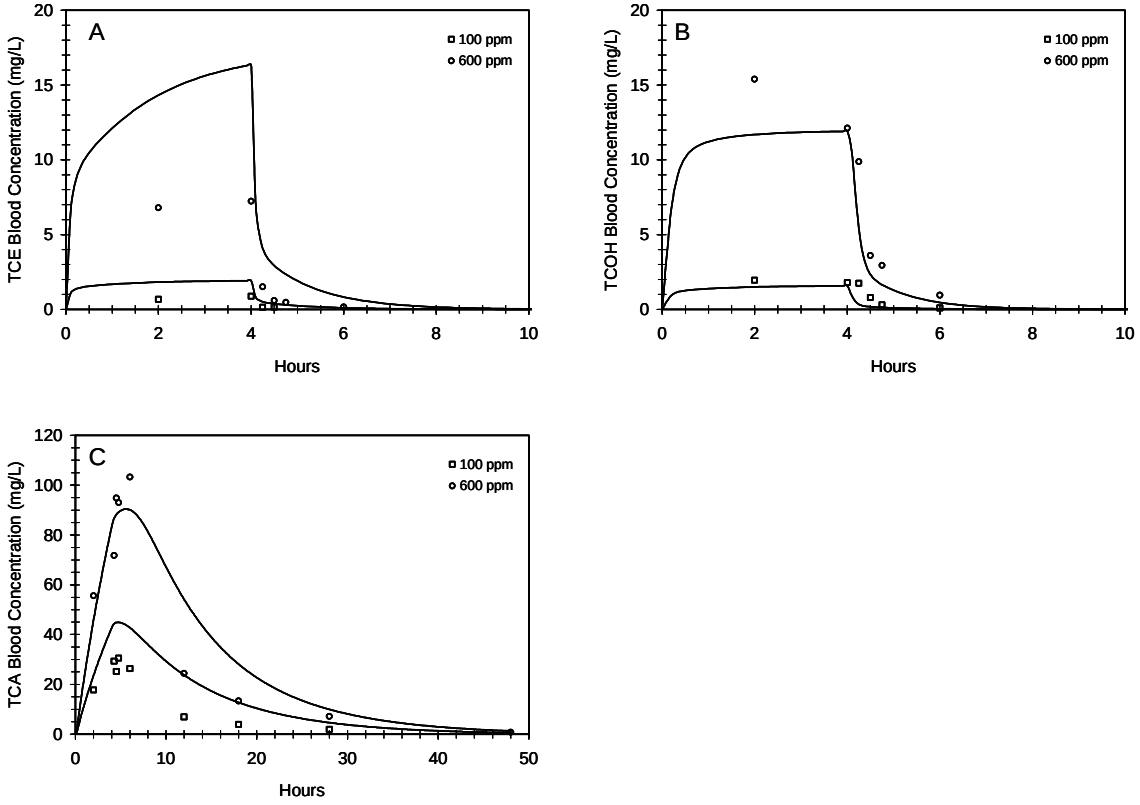

Figure 8. Comparison of predicted and experimental concentrations of TCE, TCOH, and TCA in blood in male B6C3F1 mice exposed for 4 hr to 600 ppm TCE by inhalation. Kinetic data are taken from Greenberg et al.[11]

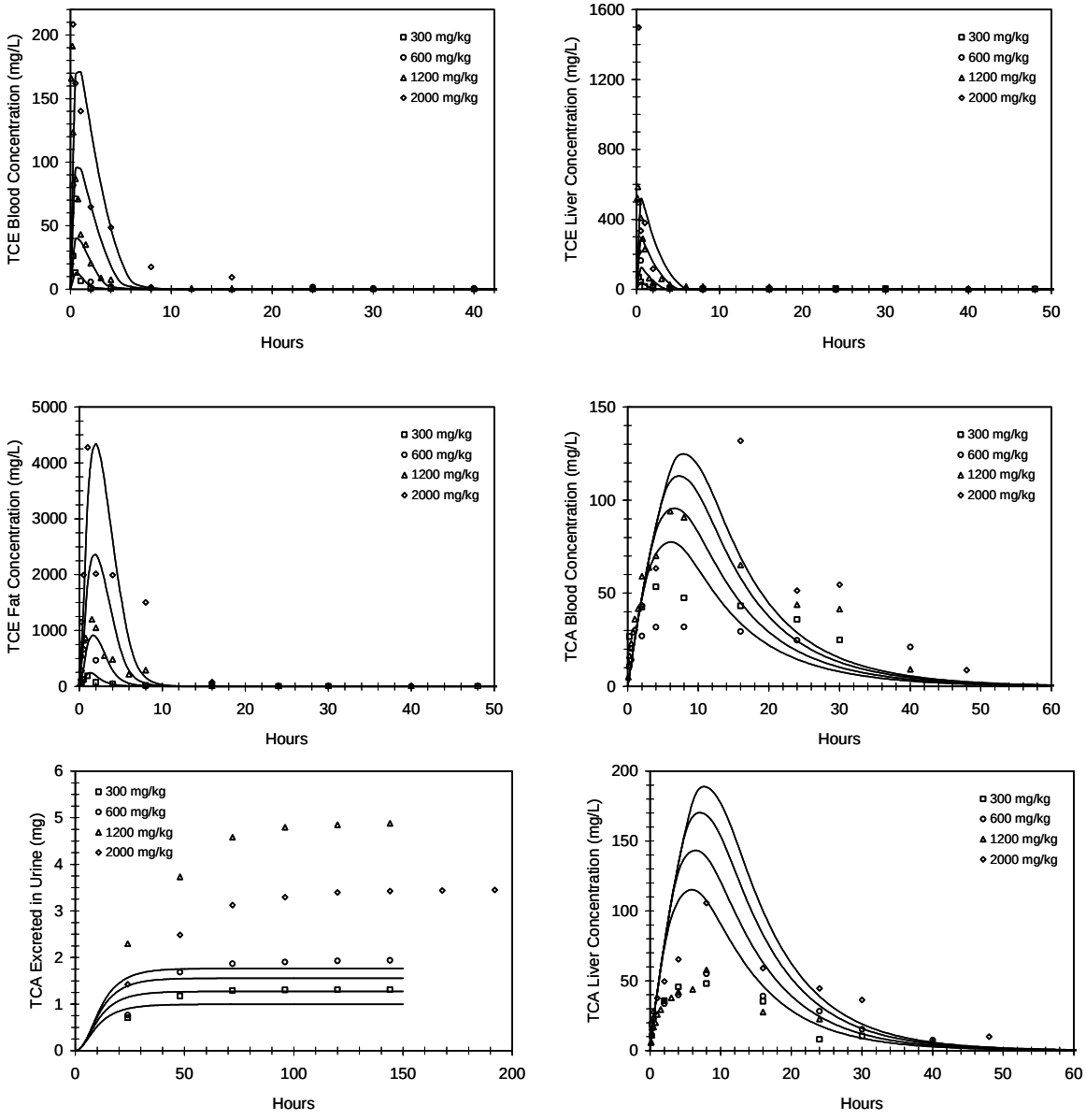

Figure 9. Comparison of predicted and experimental concentrations of TCE in blood, liver, and fat, and TCA in blood, liver, and urine in B6C3F1 mice exposed to 300, 600, 1200, and 2000 mg/kg TCE by gavage in corn oil. Kinetic data are taken from Abbas et al.[8]

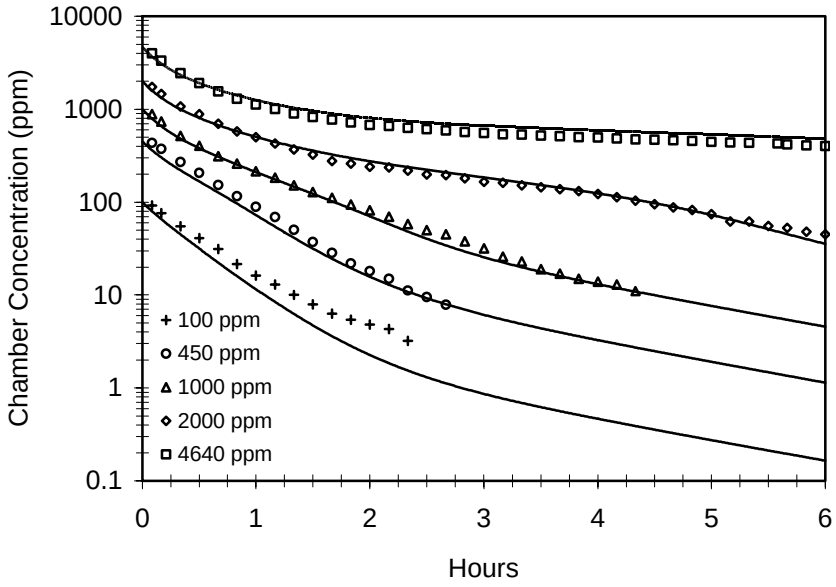

Figure 10. Comparison of predicted and experimental chamber concentrations of TCE in male F344 rats exposed to TCE in a closed, recirculating chamber. Kinetic data are taken from Andersen et al.[28]

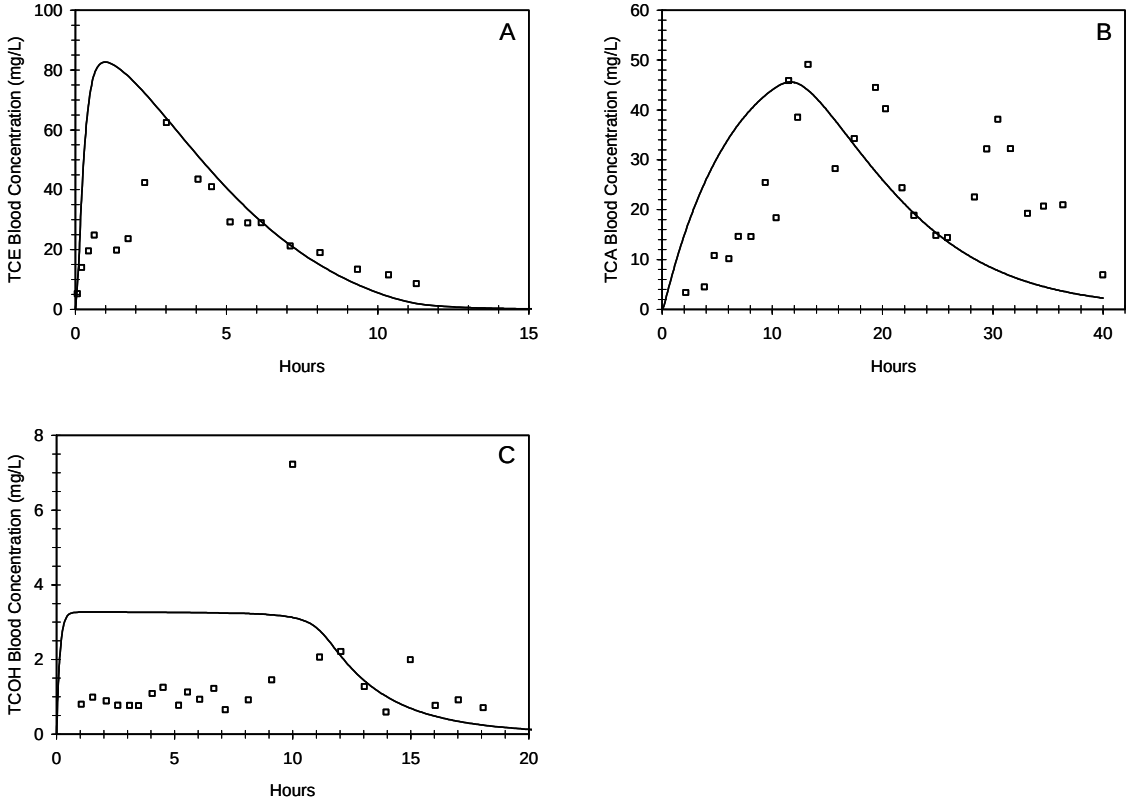

Figure 11. Mean observed and predicted blood concentrations of TCE (A), TCA (B), and free TCOH (C) following corn oil gavage with 1000 mg/kg TCE in rats. Kinetic data are taken from Prout et al.[27]

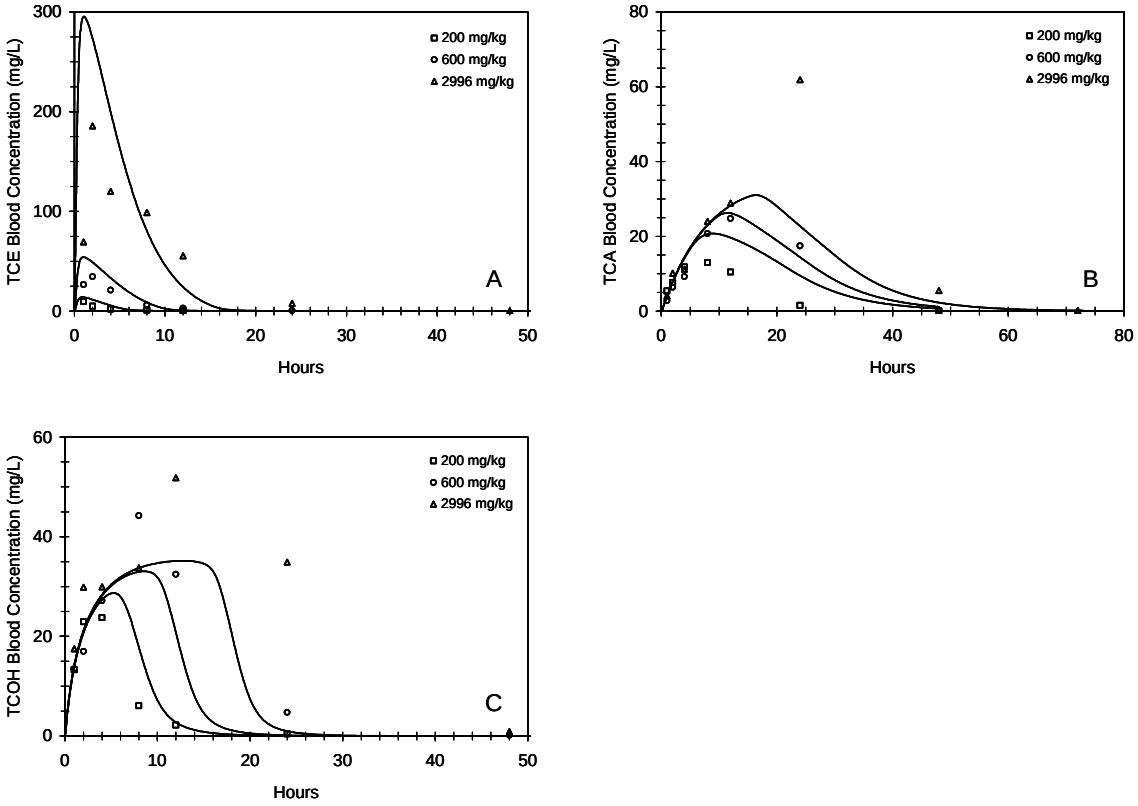

Figure 12. Mean observed and predicted blood concentrations of TCE (A), TCA (B), and free TCOH (C) following an oral doses of 200, 600, and 3000 mg/kg TCE in F-344 rats. Kinetic data are taken from Larson and Bull.[29]

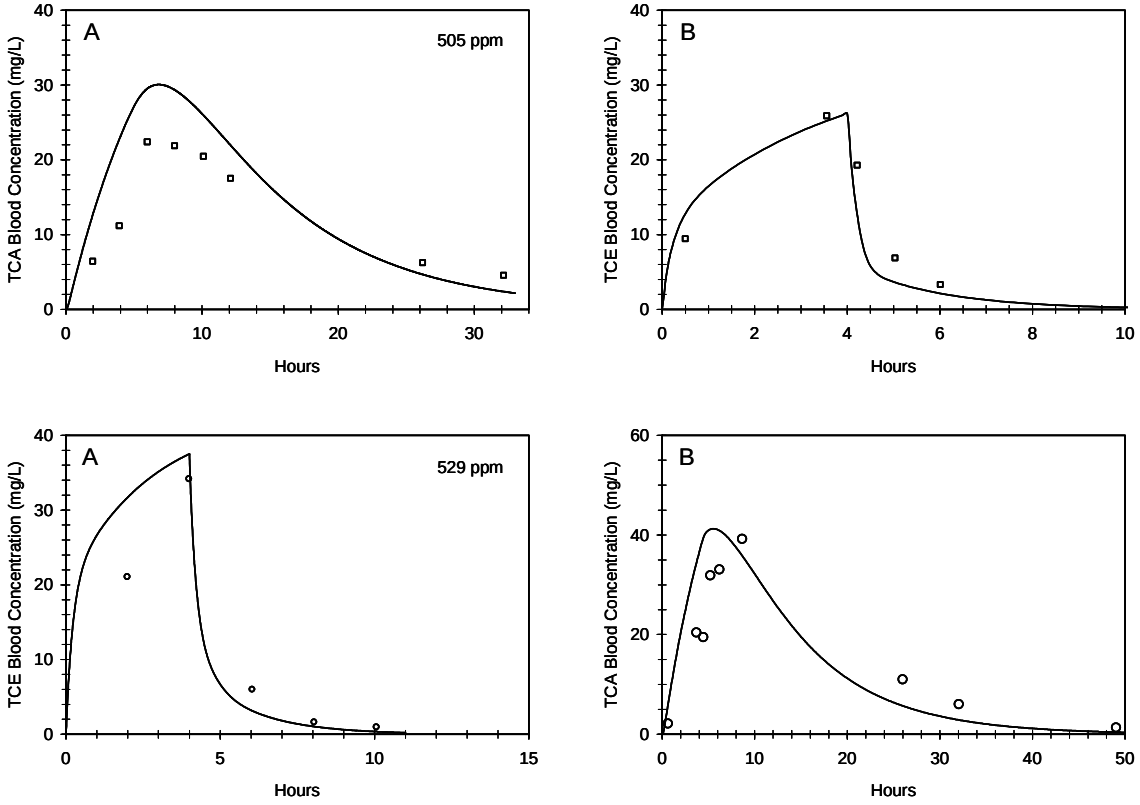

Figure 13. Comparison of predicted and experimental concentrations of TCE in blood and TCA in plasma in F-344 rats exposed to TCE by inhalation. The figures show (A) TCE blood concentrations in male rats exposed for 4 hr to 529 ppm TCE vapors and TCA plasma concentrations in male rats exposed for 4 hr to 505 ppm TCE vapors; (B) TCE blood and TCA plasma concentrations in female rats exposed for 4 hr to 600 ppm TCE vapors. Kinetic data are taken from Fisher et al.[5]

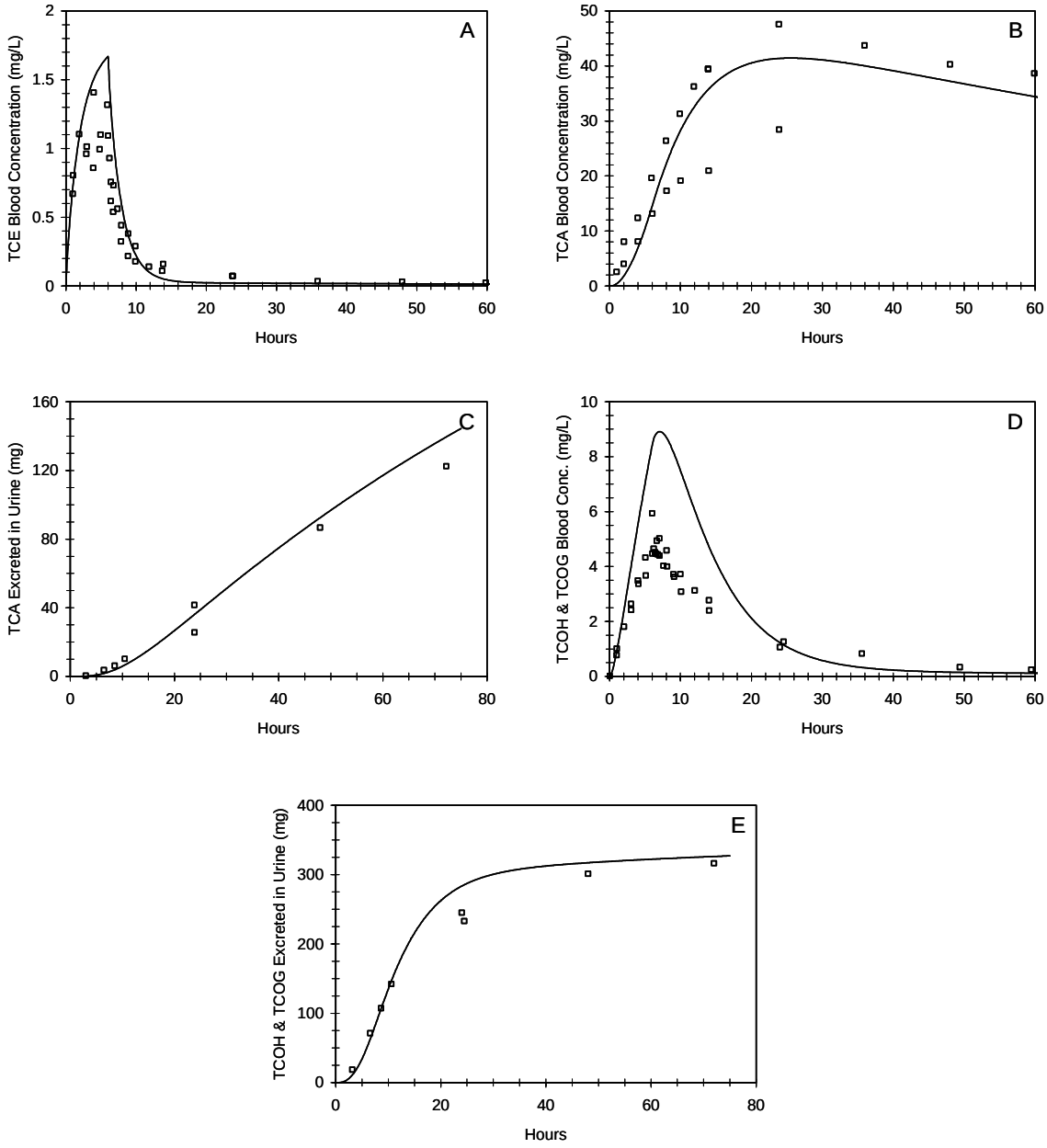

Figure 14. Mean observed and predicted kinetics of TCE and its metabolites during and after a single 6-hr exposure of human subjects to 100 ppm TCE. The simulation was obtained with VmaxC=12, VmaxTCOHC=25, kUrnTCAC=0.15, and VBodC=0.12. Kinetic data are taken from Muller et al.:[19, 30] (A) TCE blood concentrations (mg/L); (B) TCA plasma concentrations (mg/L); (C) cumulative urinary TCA excretion (mg); (D) total TCOH plasma concentrations (mg/L); (E) cumulative urinary TCOH excretion (mg).

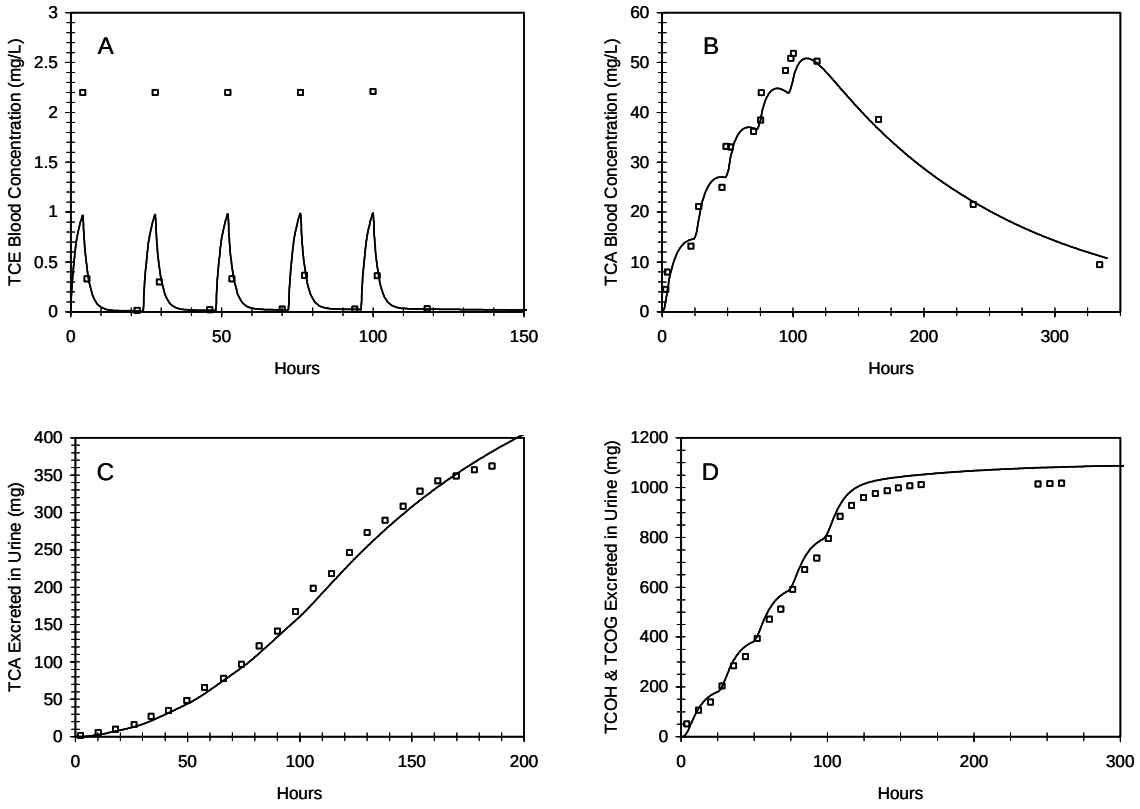

Figure 15. Mean observed and predicted kinetics of TCE and its metabolites during and after 4-hr exposures of human subjects to 70 ppm TCE for 5 days. The simulation was obtained with VmaxC=18, VmaxTCOHC=12, kUrnTCAC=0.15, and VBodC=0.12. Kinetic data are taken from Monster et al.:[31] (A) TCE venous blood concentrations (mg/L); (B) TCA plasma concentrations (mg/L); (C) cumulative urinary TCA excretion (mg); (D) cumulative urinary TCOH excretion (mg).

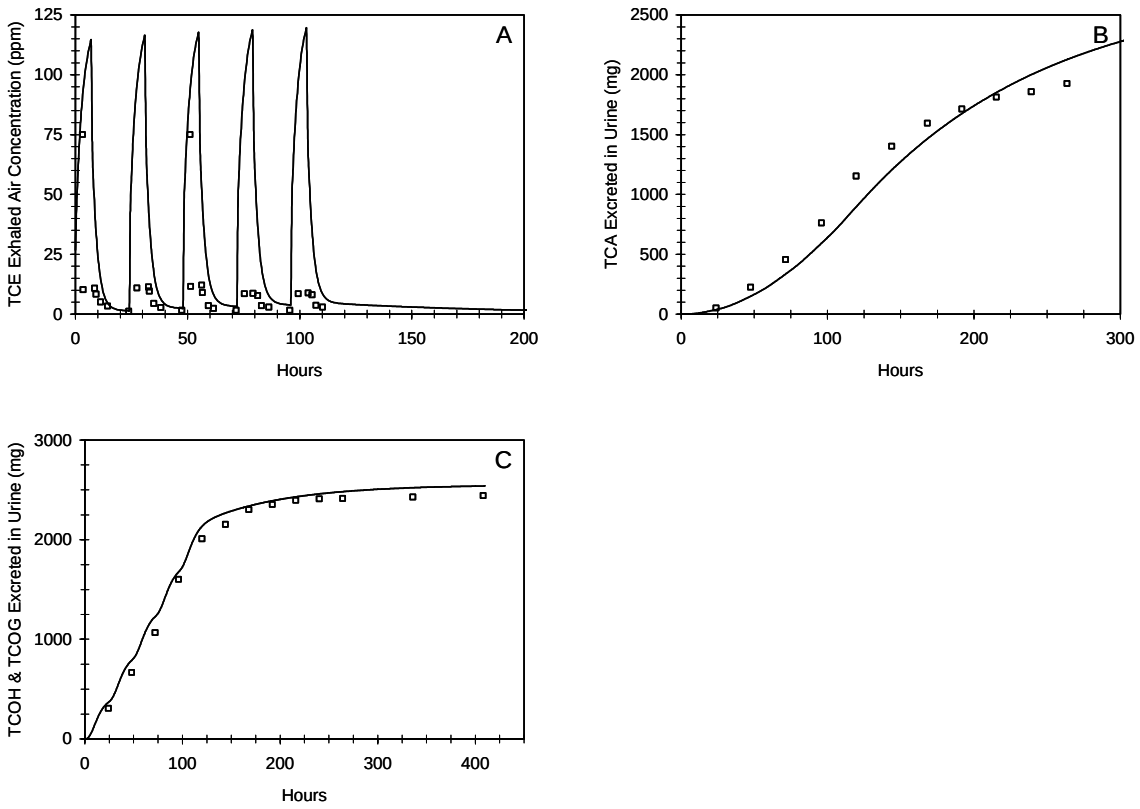

Figure 16. Mean observed and predicted kinetics of TCE and its metabolites during and following interrupted, 7-hr exposures of human subjects to 200 ppm TCE (3 hr of exposure, a one-half hour break, then 4 hr of exposure) for 5 days. The simulation was obtained with VmaxC=5, VmaxTCOHC=25, kUrnTCAC=0.2, and VBodC=0.2. Kinetic data are taken from Stewart et al.:[32] (A) TCE concentration in exhaled breath (ppm); (B) cumulative urinary TCA excretion (mg); (C) cumulative urinary TCOH excretion (mg).

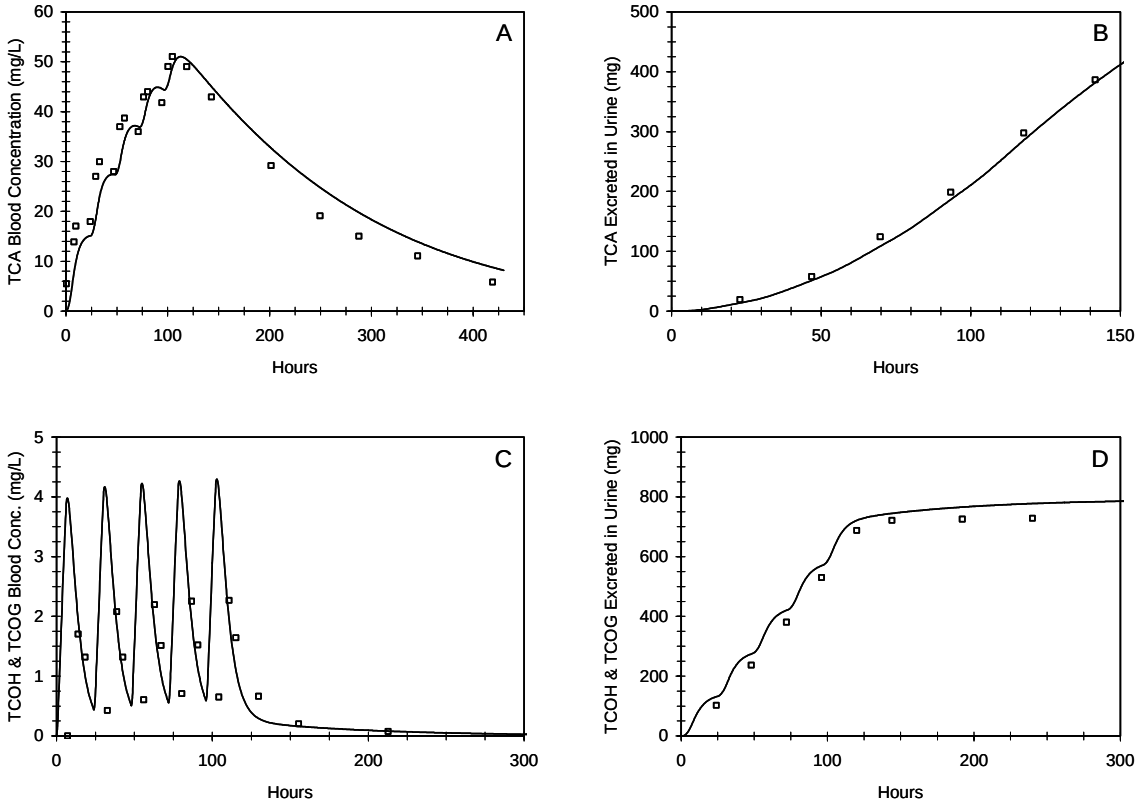

Figure 17. Mean observed and predicted kinetics of TCE and its metabolites during and after 6-hr exposures of human subjects to 50 ppm TCE for 5 days. The simulation was obtained with VmaxC=8, VmaxTCOHC=30, kUrnTCAC=0.2, and VBodC=0.2. Kinetic data are taken from Muller et al.:[30]

(A) TCA plasma concentrations (mg/L); (B) cumulative urinary TCA excretion (mg); (C) total TCOH plasma concentrations (mg/L); (D) cumulative urinary TCOH excretion (mg).

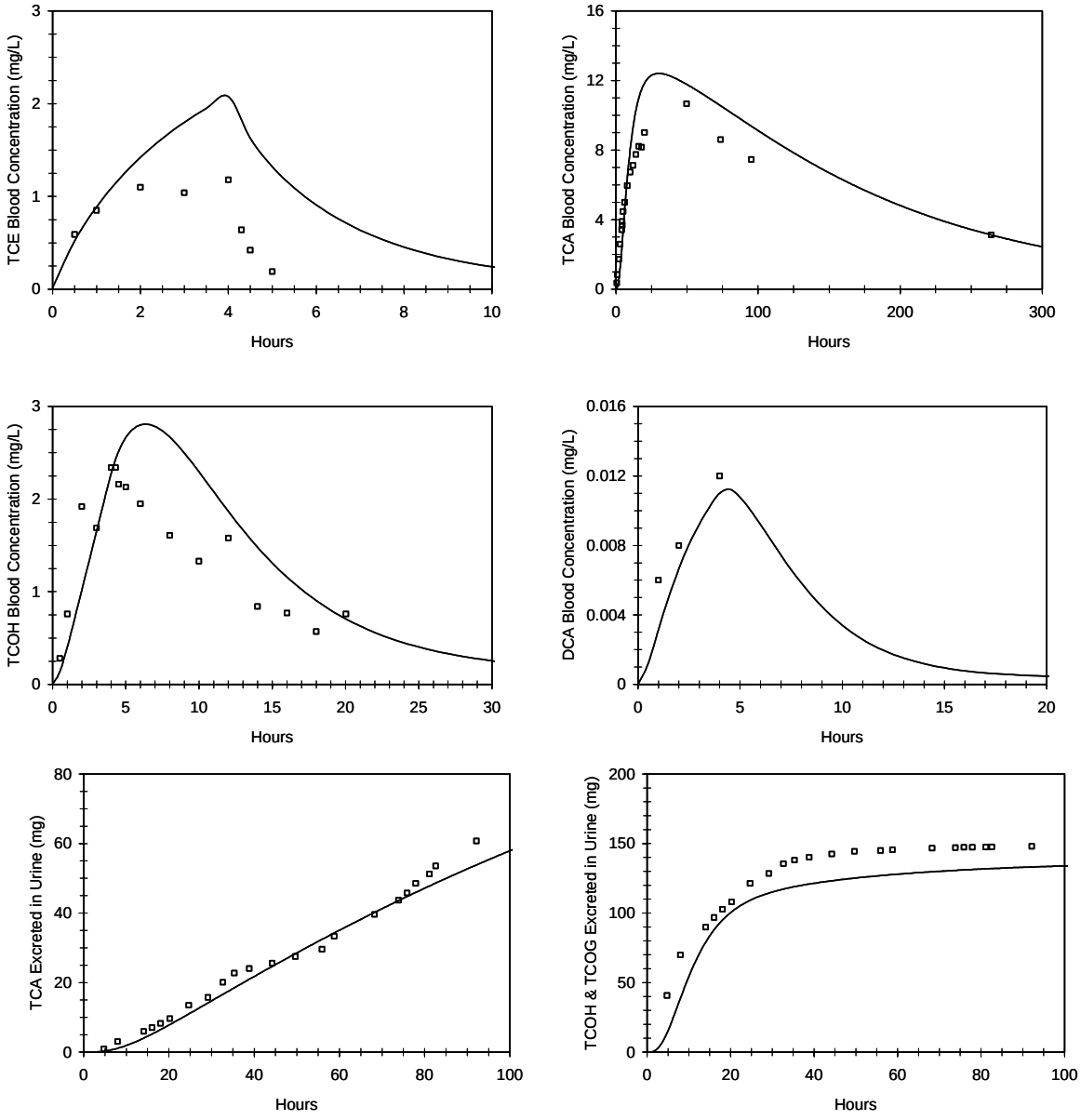

Figure 18. Observed and predicted kinetics of TCE and its metabolites TCA, TCOH, and DCA, as well as urinary excretion of TCA and TCOH, during and after a 4-hr exposures of a male human subject to 100 ppm TCE. The simulation was obtained with VmaxC=3, VmaxTCOHC=25, kUrnTCAC=0.2, and VBodC=0.2. Kinetic data are taken from Fisher et al.:[9]

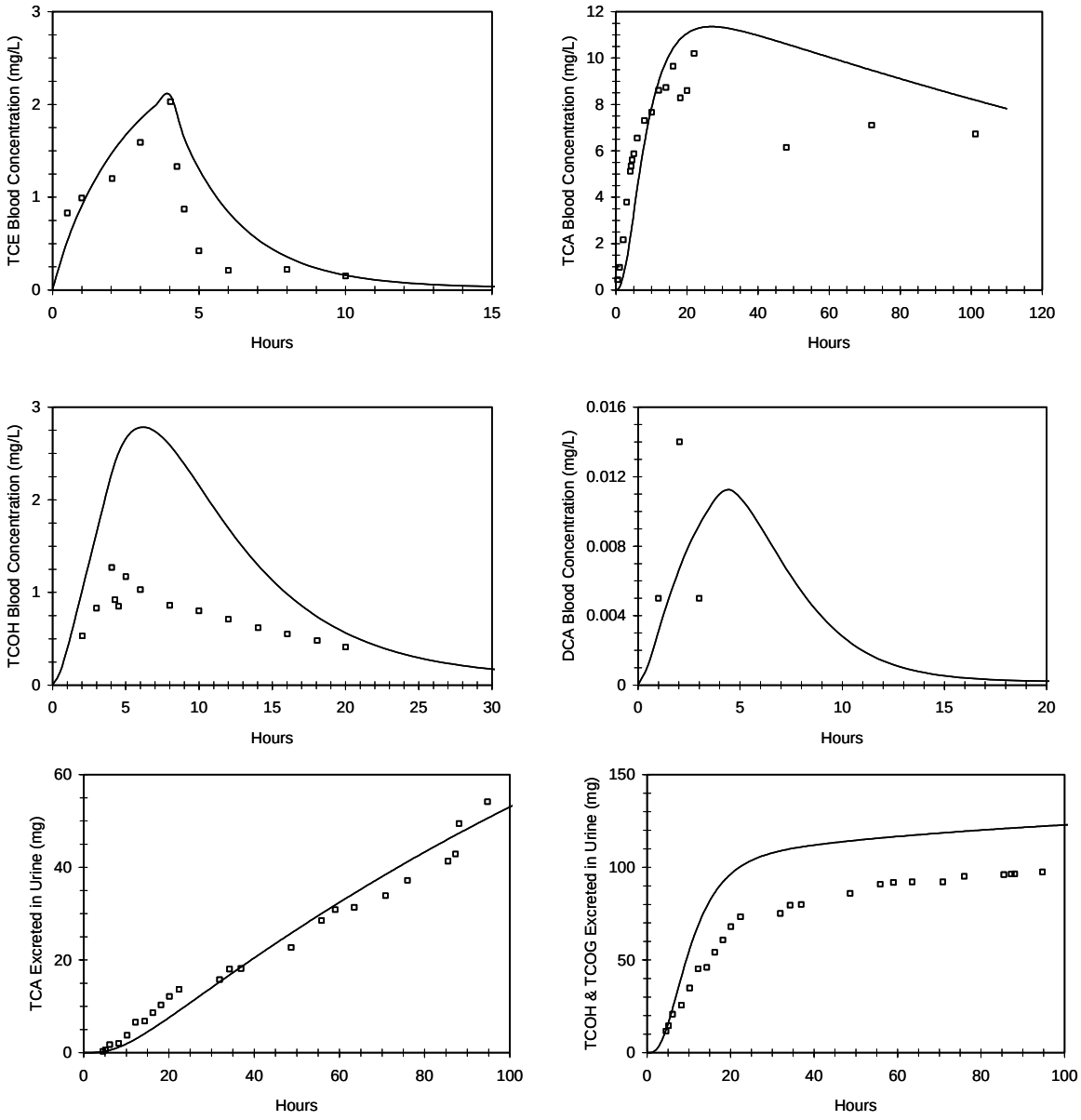

Figure 19. Observed and predicted kinetics of TCE and its metabolites TCA, TCOH, and DCA, as well as urinary excretion of TCA and TCOH, during and after a 4-hr exposures of a female human subject to 100 ppm TCE. The simulation was obtained with VmaxC=3, VmaxTCOHC=35, kUrnTCAC=0.2, and VBodC=0.2. Kinetic data are taken from Fisher et al.:[9]

Table 1: Model Parameters

		Mouse		Rat		Human	
Parameter		Value	Reference	Value	Reference	Value	Reference
BW	Body Wt (kg)	0.035 [1]	EPA default	0.35 [1]	EPA default	70.0 [1]	ICRP (International Commision on Radiological Protection (ICRP) 1975)
QCC	Cardiac output	18.0	USEPA (U.S. Environmental Protection Agency (USEPA) 1988)	15.0	Brown et al. (Brown, Delp et al. 1997)	13.0	Brown et al. (Brown, Delp et al. 1997)
QPC	Pulmonary ventilation	30.0 [2]	Brown et al. (Brown, Delp et al. 1997)	24.0 [3]	Brown et al. (Brown, Delp et al. 1997)	18.0	Astrand and Rodahl (Astrand and Rodahl 1970)
QFatC	Fat	0.07	Rat value	0.07	Brown et al. (Brown, Delp et al. 1997)	0.052	Brown et al. (Brown, Delp et al. 1997)
QGutC	Gut	0.141	Brown et al. (Brown, Delp et al. 1997)	0.162	Brown et al. (Brown, Delp et al. 1997)	0.181	Brown et al. (Brown, Delp et al. 1997)
QLivC	Liver	0.02	Brown et al. (Brown, Delp et al. 1997)	0.021	Brown et al. (Brown, Delp et al. 1997)	0.046	Brown et al. (Brown, Delp et al. 1997)
QRapC	Rapidly perfused tissues	0.713	Brown et al. (Brown, Delp et al. 1997)	0.594	Brown et al. (Brown, Delp et al. 1997)	0.699	Brown et al. (Brown, Delp et al. 1997)
QSlwC	Slowly perfused tissues	0.287	Brown et al. (Brown, Delp et al. 1997)	0.406	Brown et al. (Brown, Delp et al. 1997)	0.301	Brown et al. (Brown, Delp et al. 1997)
QTBC	Tracheo-bronchial	0.005	Brown et al. (Brown, Delp et al. 1997)	0.021	Brown et al. (Brown, Delp et al. 1997)	0.025	Brown et al. (Brown, Delp et al. 1997)
VBldC	Blood	0.049	Brown et al. (Brown, Delp et al. 1997)	0.074	Brown et al. (Brown, Delp et al. 1997)	0.079	Brown et al. (Brown, Delp et al. 1997)
VBodC	Total body	0.2	Fit to data from Fisher et al. (Fisher, Gargas et al. 1991)	0.2	Fit to data from Fisher et al. (Fisher, Gargas et al. 1991)	0.2 [3]	Fit to data from Muller et al. (Muller, Spassovski et al. 1974), (Muller, Spassovski et al. 1975)

VFatBldC	Fraction of fat that is blood	0.02	Human value	0.02	Human value	0.02	Brown et al. (Brown, Delp et al. 1997)
VFatC	Fat	0.07 [3]	Brown et al. (Brown, Delp et al. 1997)	0.07	Brown et al. (Brown, Delp et al. 1997)	0.214	Brown et al. (Brown, Delp et al. 1997)
VGutC	Gut	0.042	Brown et al. (Brown, Delp et al. 1997)	0.027	Brown et al. (Brown, Delp et al. 1997)	0.017	Brown et al. (Brown, Delp et al. 1997)
VKidC	Kidney	0.017	Brown et al. (Brown, Delp et al. 1997)	0.007	Brown et al. (Brown, Delp et al. 1997)	0.004	Brown et al. (Brown, Delp et al. 1997)
VLivC	Liver	0.055	Brown et al. (Brown, Delp et al. 1997)	0.034	Brown et al. (Brown, Delp et al. 1997)	0.026	Brown et al. (Brown, Delp et al. 1997)
VRapC	Rapidly perfused tissues	0.217	Brown et al. (Brown, Delp et al. 1997)	0.213	Brown et al. (Brown, Delp et al. 1997)	0.192	Brown et al. (Brown, Delp et al. 1997)
VSlwC	Slowly perfused tissues	0.619	Brown et al. (Brown, Delp et al. 1997)	0.664	Brown et al. (Brown, Delp et al. 1997)	0.651	Brown et al. (Brown, Delp et al. 1997)
VTBC	Tracheo-bronchial	0.0007	Brown et al. (Brown, Delp et al. 1997); Clewell et al. (Clewell, Gentry et al. 2000)	0.0005	Brown et al. (Brown, Delp et al. 1997); Clewell et al. (Clewell, Gentry et al. 2000)	0.0008	Brown et al. (Brown, Delp et al. 1997)
VDDCAC	DCA	0.5	Schultz et al. (Schultz, Merdink et al. 2002)	0.5	Saghir and Schultz (Saghir and Schultz 2003)	0.26	Curry et al. (Curry, Chu et al. 1985)
VDTCOHC	TCOH	0.65	Clewell et al. (Clewell, Gentry et al. 2000)	0.65	Clewell et al. (Clewell, Gentry et al. 2000)	0.65	Clewell et al. (Clewell, Gentry et al. 2000)
PB	Blood/air	14.0	Fisher et al. (Fisher, Gargas et al. 1991)	18.5	Fisher et al. (Fisher, Gargas et al. 1991)	9.2	Allen and Fisher (Allen and Fisher 1993)
PFat	Fat/blood	36.0	Fisher et al. (Fisher, Gargas et al. 1991)	27.5	Fisher et al. (Fisher, Gargas et al. 1991)	73.0	Allen and Fisher (Allen and Fisher 1993)
PGut	Gut/blood	1.8	Fisher et al. (Fisher, Gargas et al. 1991)	1.3	Fisher et al. (Fisher, Gargas et al. 1991)	6.8	Allen and Fisher (Allen and Fisher 1993)
PLiv	Liver/blood	1.8	Fisher et al. (Fisher, Gargas et al. 1991)	1.3	Fisher et al. (Fisher, Gargas et al. 1991)	6.8	Allen and Fisher (Allen and Fisher 1993)

PRap	Rapidly perfused/blood	1.8	Fisher et al. (Fisher, Gargas et al. 1991)	1.3	Fisher et al. (Fisher, Gargas et al. 1991)	6.8	Allen and Fisher (Allen and Fisher 1993)
PSlw	Slowly perfused/blood	0.75	Fisher et al. (Fisher, Gargas et al. 1991)	0.5	Fisher et al. (Fisher, Gargas et al. 1991)	2.3	Allen and Fisher (Allen and Fisher 1993)
PTB	TB/blood	1.8	Fisher et al. (Fisher, Gargas et al. 1991)	1.3	Fisher et al. (Fisher, Gargas et al. 1991)	6.8	Allen and Fisher (Allen and Fisher 1993)
PAFatC1	Takeup	10.0	Set to over ride two-compartment fat	10.0	Set to over ride two-compartment fat	10.0	Set to over ride two-compartment fat
PAFatC2	Release	10.0	Set to over ride two-compartment fat	10.0	Set to over ride two-compartment fat	10.0	Set to over ride two-compartment fat
PBodTCA	Body/free plasma	0.76	Abbas and Fisher (Abbas and Fisher 1997); Lumpkin et al. (Lumpkin, Dallas et al. 2003)	0.51	Jepson et al. (Jepson, Hoover et al. 1994); Lumpkin et al. (Lumpkin, Dallas et al. 2003)	1.9	Fisher et al. (Fisher, Mahle et al. 1998); Lumpkin et al. (Lumpkin, Dallas et al. 2003)
PLivTCA	Liver/free plasma	1.14	Abbas and Fisher (Abbas and Fisher 1997); Lumpkin et al. (Lumpkin, Dallas et al. 2003)	0.76	Jepson et al. (Jepson, Hoover et al. 1994); Lumpkin et al. (Lumpkin, Dallas et al. 2003)	2.5	Fisher et al. (Fisher, Mahle et al. 1998); Lumpkin et al. (Lumpkin, Dallas et al. 2003)
VMaxC	Oxidative capacity (mg/hr)	32.7 [3]	Fisher et al. (Fisher, Gargas et al. 1991)	11.2 [3]	Fisher et al. (Fisher, Gargas et al. 1991)	12.0 [3]	Allen and Fisher (Allen and Fisher 1993)
KM	Oxidative affinity (mg/L)	0.25	Fisher et al. (Fisher, Gargas et al. 1991)	0.25 [3]	Fisher et al. (Fisher, Gargas et al. 1991)	1.5	Allen and Fisher (Allen and Fisher 1993)
kDCVCC	Production of DCVC(/hr)	0.015 [4]	Clewell et al. (Clewell, Gentry et al. 2000)	0.015 [4]	Clewell et al. (Clewell, Gentry et al. 2000)	0.015 [4]	Clewell et al. (Clewell, Gentry et al. 2000)
FracDCA	Fractional split of TCE to DCA	0.04	Fit to data from Templin et al. (Templin, Parker et al. 1993)	0.04	Mouse value	0.004	Fit to data from Fisher et al. (Fisher, Mahle et al. 1998)

FracTCE	Fractional split of TCE to TCA	0.035	Fit to data from Prout et al. (Prout, Provan et al. 1985)	0.04 [3]	Fisher et al. (Fisher, Gargas et al. 1991)	0.08 [4]	Clewell et al. (Clewell, Gentry et al. 2000)
VMaxClaraC	VMax	3.0	Clewell et al. (Clewell, Gentry et al. 2000)	0.3	Clewell et al. (Clewell, Gentry et al. 2000)	0.0045	Clewell et al. (Clewell, Gentry et al. 2000)
KMClara	KM	0.25	Clewell et al. (Clewell, Gentry et al. 2000)	0.25	Clewell et al. (Clewell, Gentry et al. 2000)	1.5	Clewell et al. (Clewell, Gentry et al. 2000)
VMaxClearC	VMax for chloral clearance	250.0	Clewell et al. (Clewell, Gentry et al. 2000)	250.0	Clewell et al. (Clewell, Gentry et al. 2000)	250.0	Clewell et al. (Clewell, Gentry et al. 2000)
KMClear	KM for chloral clearance	250.0	Clewell et al. (Clewell, Gentry et al. 2000)	250.0	Clewell et al. (Clewell, Gentry et al. 2000)	250.0	Clewell et al. (Clewell, Gentry et al. 2000)
kDissoc	Protein/TCA dissociation constant (µmole/L)	46.1	Lumpkin et al. (Lumpkin, Dallas et al. 2003)	383.6	Lumpkin et al. (Lumpkin, Dallas et al. 2003)	174.6	Lumpkin et al. (Lumpkin, Dallas et al. 2003)
NumSites	Number of binding sites per class protein	0.17	Lumpkin et al. (Lumpkin, Dallas et al. 2003)	1.49	Lumpkin et al. (Lumpkin, Dallas et al. 2003)	2.97	Lumpkin et al. (Lumpkin, Dallas et al. 2003)
ProtConc	Protein concentration (µmoles/L)	196.0	Lumpkin et al. (Lumpkin, Dallas et al. 2003)	190.0	Lumpkin et al. (Lumpkin, Dallas et al. 2003)	239.0	Lumpkin et al. (Lumpkin, Dallas et al. 2003)
VMaxTCOHC	VMax for oxidation to TCA	1.0 [3, 4]	Clewell et al. (Clewell, Gentry et al. 2000)	0.12 [3, 4]	Clewell et al. (Clewell, Gentry et al. 2000)	25.0 [3,4]	Clewell et al. (Clewell, Gentry et al. 2000)
KMTCOH	KM for oxidation to TCA	0.25 [4]	Clewell et al. (Clewell, Gentry et al. 2000)	0.25 [4]	Clewell et al. (Clewell, Gentry et al. 2000)	250.0 [4]	Clewell et al. (Clewell, Gentry et al. 2000)
VMaxGlucC	VMax for glucuronidation to TCOG	100.0 [4]	Clewell et al. (Clewell, Gentry et al. 2000)	100.0 [3,4]	Clewell et al. (Clewell, Gentry et al. 2000)	5.0 [4]	Clewell et al. (Clewell, Gentry et al. 2000)
KMGluc	KM for glucuronidation to TCOG	25.0 [4]	Clewell et al. (Clewell, Gentry et al. 2000)	25.0 [4]	Clewell et al. (Clewell, Gentry et al. 2000)	25.0 [4]	Clewell et al. (Clewell, Gentry et al. 2000)

kNATC	Clearance of DCVC by NAT	0.5 [4]	Clewell et al. (Clewell, Gentry et al. 2000)	1.1	Clewell et al. (Clewell, Gentry et al. 2000)	19.0	Clewell et al. (Clewell, Gentry et al. 2000)
kKidCytoC	Kidney cytotoxicity from DCVC	0.4 [4]	Clewell et al. (Clewell, Gentry et al. 2000)	17.0	Clewell et al. (Clewell, Gentry et al. 2000)	37.0	Clewell et al. (Clewell, Gentry et al. 2000)
kAS	Stomach to gut	0.0 [4]	Clewell et al. (Clewell, Gentry et al. 2000)	0.0 [4]	Clewell et al. (Clewell, Gentry et al. 2000)	0.0 [4]	Clewell et al. (Clewell, Gentry et al. 2000)
kTSD	Stomach to duodenum	10.0 [4]	Clewell et al. (Clewell, Gentry et al. 2000)	10.0 [4]	Clewell et al. (Clewell, Gentry et al. 2000)	10.0 [4]	Clewell et al. (Clewell, Gentry et al. 2000)
kAD	Duodenum to liver	0.6 [3]	Fit to data from Prout et al. (Prout, Provan et al. 1985)	0.3 [3]	Fit to data from Templin et al. (Templin, Stevens et al. 1995)	1.0 [4]	Clewell et al. (Clewell, Gentry et al. 2000)
kTD	Fecal excretion	0.0 [4]	Clewell et al. (Clewell, Gentry et al. 2000)	0.0 [4]	Clewell et al. (Clewell, Gentry et al. 2000)	0.0 [4]	Clewell et al. (Clewell, Gentry et al. 2000)
kBileC	Biliary excretion of TCOG	1.0 [4]	Clewell et al. (Clewell, Gentry et al. 2000)	1.0 [4]	Clewell et al. (Clewell, Gentry et al. 2000)	1.0 [4]	Clewell et al. (Clewell, Gentry et al. 2000)
kEHRC	Enterohepatic recirculation of TCOH	0.0 [4]	Clewell et al. (Clewell, Gentry et al. 2000)	0.0 [3,4]	Clewell et al. (Clewell, Gentry et al. 2000)	0.0 [4]	Clewell et al. (Clewell, Gentry et al. 2000)
kClearDCAC	Clearance of DCA	1.0	Schultz et al. (Schultz, Merdink et al. 2002)	1.3	Saghir and Schultz (Saghir and Schultz 2003)	1.9	Curry et al. (Curry, Chu et al. 1985)
kUrnTCAC	Urinary excretion of TCA	0.3 [3]	Fit to data from Fisher et al. (Fisher, Gargas et al. 1991)	0.3	Fit to data from Fisher et al. (Fisher, Gargas et al. 1991)	0.2 [3]	Fit to data from Muller et al. (Muller, Spassovski et al. 1974), (Muller, Spassovski et al. 1975)
kUrnTCOGC	Urinary excretion of TCOG	0.5 [4]	Clewell et al. (Clewell, Gentry et al. 2000)	0.5 [4]	Clewell et al. (Clewell, Gentry et al. 2000)	3.0 [4]	Clewell et al. (Clewell, Gentry et al. 2000)

FracPlas	Fraction of blood that is plasma	0.58	Human value	0.58	Human value	0.58	ICRP (International Commision on Radiological Protection (ICRP) 1975)
TCAPlas	To convert TCA in plasma to TCA in blood	0.76	Personal communication with Jeff Fisher	0.76	Personal communication with Jeff Fisher	0.76	Personal communication with Jeff Fisher

[1] Used study specific values when available.
[2] 18.0 was used for open chamber simulations. 30.0 was used for closed chamber simulations.
[3] Different values were needed to fit some data sets.
[4] Value from Clewell et al. (Clewell, Gentry et al. 2000) was fit to data.

Abbas, R. and J. W. Fisher (1997). "A physiologically based pharmacokinetic model for trichloroethylene and its metabolites, chloral hydrate, trichloroacetate, dichloroacetate, trichloroethanol, and trichloroethanol glucuronide in B6C3F1 mice." Toxicol. Appl. Pharmacol. **147**: 15-30.

Allen, B. D. and J. W. Fisher (1993). "Pharmacokinetic modeling of trichloroethylene and trichloroacetic acid in humans." Risk Anal. **13**: 71-86.

Astrand, P. and K. Rodahl (1970). Textbook of Work Physiology. New York, NY, McGraw-Hill.

Brown, R. P., M. D. Delp, et al. (1997). "Physiological parameter values for physiologically based pharmacokinetic models." Toxicol Ind Health **13**: 407-484.

Clewell, H. J., P. R. Gentry, et al. (2000). "Development of a physiologically based pharmacokinetic model of trichloroethylene and its metabolites for use in risk assessment." Environ. Health Perspect. **108**((suppl 2)): 283-305.

Curry, S. H., P.-I. Chu, et al. (1985). "Plasma concentrations and metabolic effects of intravenous sodium dichloroacetate." Clin. Pharmacol. Ther. **37**: 89-93.

Fisher, J. W., M. L. Gargas, et al. (1991). "Physiologically based pharmacokinetic modeling with trichloroethylene and its metabolite, trichloroacetic acid, in the rat and mouse." Toxicol. Appl. Pharmacol. **109**: 183-195.

Fisher, J. W., D. A. Mahle, et al. (1998). "A human physiologically based pharmacokinetic model for trichloroethylene and its metabolites, trichloroacetic acid and free trichloroethanol." Toxicol. Appl. Pharmacol. **152**: 339-359.

International Commision on Radiological Protection (ICRP) (1975). Report of the Task Group on Reference Man. Oxford, Pergamon Press.

Jepson, G. W., D. K. Hoover, et al. (1994). "A partition coefficient determination method for nonvolatile chemicals in biological tissues." Fundamental and Applied Toxicology **22**: 519-524.

Lumpkin, M. H., C. E. Dallas, et al. (2003). "Physiologically based pharmacokinetic modeling of species-specific effects of plasma binding of trichloroacetic acid from trichloroethylene in mice, rats, and humans." Toxicologist **72**(S-1): 867.

Muller, G., M. Spassovski, et al. (1974). "Metabolism of trichloroethylene in man. II. Pharmacokinetics of metabolites." Arch. Toxikol. **32**: 283-295.

Muller, G., M. Spassovski, et al. (1975). "Metabolism of trichloroethylene in man. III. Interaction of trichloroethylene and ethanol." Arch. Toxikol. **33**: 173-189.

Prout, M. S., W. M. Provan, et al. (1985). "Species differences in response to trichloroethylene." Toxicol. Appl. Pharmacol. **79**: 389-400.

Saghir, S. A. and I. R. Schultz (2003). "Low-dose pharmacokinetics and oral bioavailability of dichloroacetate in naive and GST-zeta-depleted rats." Environ Health Perspect **110**(8): 757-63.

Schultz, I. R., J. L. Merdink, et al. (2002). "Dichloroacetate toxicokinetics and disruption of tyrosine catabolism in B6C3F1 mice: dose-response relationships and age as a modifying factor." Toxicology **173**(3): 229-47.

Templin, M. V., J. C. Parker, et al. (1993). "Relative formation of dichloroacetate and trichloroacetate from trichloroethylene in male B6C3F1 mice." Toxicol. Appl. Pharmacol. **123**: 1-8.

Templin, M. V., D. K. Stevens, et al. (1995). "Factors affecting species differences in the kinetics of metabolites of trichloroethylene." J. Toxicol. Environ. Health **44**: 435-447.

U.S. Environmental Protection Agency (USEPA) (1988). Reference physiological parameters in pharmacokinetic modeling. Washington, DC, Office of Research and Development.